FLEXURAL STIFFNESS OF PARTIALLY ENCASED COMPOSITE COLUMNS IN MAJOR AXIS BENDING

MURTAZA MUHAMMAD SHAHRIAR

STUDENT NO. 100704341

MASTER OF SCIENCE IN CIVIL & STRUCTURAL ENGINEERING

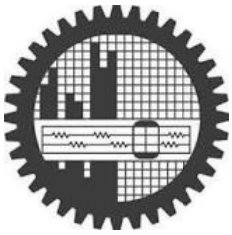

DEPARTMENT OF CIVIL ENGINEERING

BANGLADESH UNIVERSITY OF ENGINEERING AND TECHNOLOGY

DHAKA, BANGLADESH

MAY, 2014

FLEXURAL STIFFNESS OF PARTIALLY ENCASED COMPOSITE COLUMNS IN MAJOR AXIS BENDING

SUBMITTED BY

MURTAZA MUHAMMAD SHAHRIAR

STUDENT NO. 100704341

A Thesis Submitted in Partial Fulfillment of the Requirements for the Degree of Master of Science in Civil & Structural Engineering

DEPARTMENT OF CIVIL ENGINEERING

BANGLADESH UNIVERSITY OF ENGINEERING AND TECHNOLOGY

DHAKA, BANGLADESH

MAY, 2014

CERTIFICATE OF APPROVAL

The thesis titled **"Flexural Stiffness of Partially Encased Composite Columns in Major Axis Bending"** submitted by Murtaza Muhammad Shahriar, Student number 100704341P, Session: October 2007 has been accepted as satisfactory in partial fulfilment of the requirements for the degree of Master of Science in Engineering (Civil & Structural) on 21st May 2014.

BOARD OF EXAMINERS

1. **Dr. Mahbuba Begum** — **Chairman**
   Associate Professor (Supervisor)
   Department of Civil Engineering,
   BUET, Dhaka.

2. **Dr. A.M.M. Taufiqul Anwar** — **Member**
   Professor & Head (Ex-officio)
   Department of Civil Engineering,
   BUET, Dhaka.

3. **Dr. Sk. Sekender Ali** — **Member**
   Professor
   Department of Civil Engineering
   BUET, Dhaka.

4. **Dr. Khan Mahmud Amanat** — **Member**
   Professor
   Department of Civil Engineering
   BUET, Dhaka.

5. **Dr. M. Shamim Z. Bosunia** — **Member**
   Ex-Professor, Dept. of CE, BUET (External)
   Apt. 501, House 62, Road-27, Gulshan.

ACKNOWLEDGEMENT

In the name of Allah, the most Gracious and the most Merciful

The author sincerely expresses his deepest gratitude to the Almighty.

Foremost, the author would like to thank and express his gratefulness to his supervisor Dr. Mahbuba Begum, Associate Professor, Department of Civil Engineering, Bangladesh University of Engineering and Technology (BUET) for allowing him to do this work and for her overall support in accomplishing the research work. Her guidance on the research methods, deep knowledge, motivation, encouragement and patience in all the stages of this research work has been made the task of the author less difficult and made it possible to complete the thesis work.

The author's sincere appreciation goes to his parents, wife and other family members who gave him endless inspiration and support without which it would be quite impossible to complete this work.

The deepest gratitude goes to the head of the department who allowed the author an extension of time for this thesis work without which the completion of this work would never be possible by the author.

ABSTRACT

Partially encased composite (PEC) column is a comparatively new type of composite column which consists of a thin-walled welded I shaped steel section with transverse links welded between the opposing flanges. The space between the flanges and the web is filled with concrete. Previously no substantial study has been done on effective flexural stiffness (*EI*) of PEC columns in major or minor axis of steel section. The influences of several key parameters on the slenderness behaviour of this column are yet to be investigated. Moreover, the ACI equations for *EI*, currently in use were developed for RC columns subjected to high axial loads and were simply modified, without any further investigation, for use in general composite column design. This study made an attempt to judge the applicability of this equation for the flexural stiffness of PEC columns in which steel shapes are partially encased by concrete. To this end the effective flexural stiffness of partially encased composite columns are evaluated theoretically using the slender column strength curve and the cross-sectional strength curve. Newmark's iterative procedure was implemented to evaluate the second-order deflection of slender columns which was eventually used to calculate the second-order moment for slender columns. Strain-compatibility and force equilibrium equations were used to construct the cross-sectional strength curve.

An extensive parametric study has been conducted in this research in order to observe the effects of four geometric and two material variables on the flexural stiffness *EI* of slender PEC columns subjected to short-term loads and equal end moments causing symmetrical single-curvature bending about the major axis of the encased steel section. A number of 1,200 parametric data regarding *EI* were generated in this study. This data have been compared to the existing flexural stiffness equation in ACI code. It has been found that the existing ACI equation gives satisfactorily close results at low eccentricities. But at high eccentricities, ACI equation does not give satisfactory results. A regression analysis has been conducted and a design equation was proposed to calculate the flexural stiffness of PEC columns subjected to major axis bending. This proposed equation includes the parameters *L/d* and *e/d*, that were proven to be most significant factors affecting the behaviour of PEC columns under major axis bending. The reliability of the proposed *EI* equation was tested against all the parametric data and was found to be satisfactory.

TABLE OF CONTENTS

LIST OF SYMBOLS

A_c	Cross-sectional area of concrete
A_r	Cross-sectional area of additional reinforcing steel bars
A_s	Cross-sectional area of steel shape
A_{se}	Effective cross-sectional area of steel shape
b	Unsupported flange width
b_e	Width of concrete stress block
b_f	Full flange width (equals 2b)
b/t	Width-to-thickness ratio of flange plate (plate slenderness ratio)
c	Distance between extreme compression fiber and neutral axis
C_c	Total force in concrete stress block
C_{ec}	Euler buckling load for PEC columns
C_m	Equivalent uniform moment diagram factor
C_r	Cross-sectional strength of PEC column
C_u	Design capacity of PEC columns
d	Column depth
D	Sustained dead load on column
E_c	Modulus of elasticity for concrete
E_s	Modulus of elasticity for steel
EI	Effective flexural stiffness of columns
EI_{th}	Theoretical flexural stiffness of parametric columns
EI_{ACI}	Flexural stiffness of columns calculated from ACI equations
e	Initial load eccentricity used in the parametric study
e/d	Initial load eccentricity ratio used in the parametric study
f'_c	Compressive stress of concrete
f_{cu}	Measured uniaxial compressive strength of concrete
F_y	Yield strength of steel shape
h	Column depth (=d)
I_c	Moment of inertia of concrete section
I_s, I_{ss}	Moment of inertia of steel shape

I_g	Gross moment of inertia of section
I_{rs}	Moment of inertia of reinforcing steel
k	Plate buckling coefficient, the lowest Eigen-value solution to the basic differential equation of equilibrium
KL	Effective column length
l, L	Column length
L/d	Column slenderness ratio
M_c	Design bending moment that includes second-order effects
M_{cs}	Cross sectional moment capacity
M_{col}	Actual column moment capacity
M_e	End moment of column due to eccentric loading
M_2	Maximum end moment of column
n	Empirical factor used to relate effective flange width to actual flange width, Total number of data used in statistical analysis
P	Axial Load
P_u	Peak load of column
P_c, P_{cr}	Euler's Critical buckling load
s	Link spacing of PEC column
s/d	Link spacing-to-depth ratio of PEC column
t	Plate thickness
t_f	Thickness of flange plate
t_w	Thickness of web plate
T	Total sustained load of column
α	Empirical factor to account for initial imperfections and residual stresses
α_1	Ratio of average stress in rectangular concrete compression block to concrete strength (CSA 2004c)
β_1	Ratio of depth of rectangular concrete compression block to depth to the neutral axis (CSA 2004c)
β_d	Sustained load factor taken as the ratio of the maximum factored axial dead load to the total factored axial load.
Δ	Secondary deflection of column at mid height due to slenderness effect

δ_{ns}	Moment magnifier for columns that are part of braced (non-sway) frames
δ_1	Moment magnifier for columns when subjected to axial load and equal & opposite end moments causing symmetrical single curvature bending
$\emptyset$	Curvature
λ	Column slenderness parameter
λ_p	Steel flange slenderness parameter
ν_s	Poisson's ratio for steel
ψ	Parameter to account for size effects on PEC columns

Chapter 1

INTRODUCTION

1.1 BACKGROUND

A steel-concrete composite column is a compression member, comprising either a concrete filled tubular section of hot-rolled steel or a concrete encased hot-rolled steel section. In recent years, researchers have found that the effective use of a combination of steel with concrete can substantially improve the behaviour and cost efficiency of columns used in the construction of medium to high-rise buildings, as compared to using steel-only columns. Composite columns, either encased or filled, can be an economical solution for cases where additional load capacity is desired over that available with steel columns alone. Effective composite systems combine the speed of erection of steel buildings with the relatively low material cost of concrete. Two types of composite columns commonly used in North America are: Concrete Filled Tubes (CFT) and Fully Encased Composite (FEC) Columns (Figure 1.1).

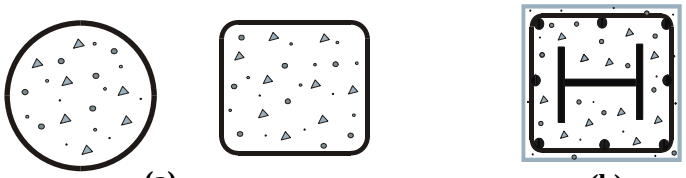

Figure 1.1: Common types of Composite columns, (a) Concrete Filled Tubes and (b) Fully Encased Composite Column.

But both of these composite systems have limitations such as limited cross-sectional dimensions of standard shapes (CFT), requirement of extensive formwork and additional reinforcing steel (FEC columns) and complex beam-to-column connections. These limitations have indirectly imposed restrictions on the use of composite columns. So the necessity of development of a new kind of composite column has become inevitable.

One of the recent developments in composite system is partially encased composite (PEC) columns. In Europe, in the early 1980s, partially encased composite (PEC) columns and beams were introduced using standard-sized rolled steel sections. In 1996, the Canam Group in Canada proposed a new type of PEC column consisting of a thin-walled, welded H-shaped steel section, built-up from hot-rolled steel plate, with concrete infill cast between the flanges consisting of a thin-walled welded I-shaped steel section. The steel section features very slender plates exceeding the width-to-thickness ratio limits for non-compact sections. Transverse links are provided between the flanges at regular intervals to enhance the resistance to local buckling. This new innovative system has been developed by the Canam Manac Group through a collaborative research project involving Canadian and American universities with a view to overcoming the limitations related to erection, connection design, and economy of more commonly used composite columns. This innovative composite system not only reduces the above mentioned cost of construction using relatively low-cost concrete by minimizing the use of higher cost steel, but also helps to overcome the complexities related to erection and design of connections of more commonly used composite columns.

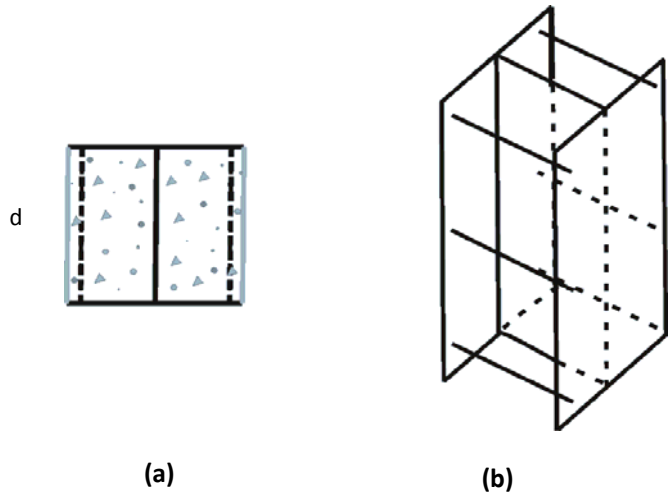

Figure 1.2: Partially Encased Composite Column with Thin-Walled Built-Up Steel Section, (a) Column Cross-Section and (b) 3D view of the Steel Configuration.

In PEC columns, since a built–up steel section is used instead of a standard shape, the designer has more flexibility when sizing the column cross-section. Moreover, thin steel plates are intentionally specified to obtain a more cost effective column by increasing the contribution of concrete in the load carrying capacity of the column. These factors have made PEC columns constructed with built-up shapes more attractive than those constructed with standard sections. Moreover, the high stiffness of the PEC column is expected to have beneficial effects for controlling the lateral deflection of buildings when used as a component of lateral load resisting systems and incorporating the use of high performance materials in the system.

Several research works including both experimental and numerical works (Tremblay *et al.* 1998; Chicoine *et al.* 2000, 2002, 2003; Bouchereau and Toupin 2003, Prickett and Driver 2006; Maranda 1998, Chicoine *et al.* 2002 and Begum *et al.* 2007) have been carried out for establishing the behaviour and design provisions for this new type of composite column under various loading conditions. Most of these research works were confined in exploring the short (length-to-depth ratio of 5) column behaviour of PEC columns. However, a few long column tests (length-to-depth ratio of 20) were carried out by Chicoine *et al.* (2003) under static loading. This test database is not sufficient to establish a design guideline for slender PEC columns. The flexural strength of a slender column subjected to end moments causing symmetrical single curvature bending is lower than the strength of its cross-section due to the second-order bending moment. The moment magnifier approach is followed in most of the codes (ACI 318-02; CSA A23.3) for computing the second-order moments in slender columns. This approach is introduced into design practice to eliminate the need for extensive calculations, based on the solution to a differential equation, to compute second-order bending moments in columns. The moment magnifier approach is greatly influenced by the critical buckling load, which again is dependent on the effective flexural stiffness of the slender column. The *EI* expressions given in ACI 318-02 (2002), for composite columns were mainly developed for reinforced concrete columns. Mirza and Tikka (2006) performed a statistical evaluation to judge the applicability of this equation for the flexural stiffness of composite columns in which steel shapes are fully encased in concrete. In

partially encased composite columns the effective flexural stiffness (*EI*) can be greatly affected by the local buckling of the thin flange plate, nonlinear stress-strain diagram of concrete, creep and cracking along the height of the column. An attempt has been made in this study to investigate the sensitivity of this equation to various geometric and material parameters of thin-walled PEC columns.

1.2 OBJECTIVES AND SCOPE OF THE STUDY

The objectives of current study are:

i) To evaluate the effective flexural stiffness (*EI*) of slender PEC columns subjected to bending about the major axis of the steel section.
ii) To determine the influence of a full range of geometric and material parameters on the effective flexural stiffness (*EI*) of slender PEC columns subjected to major axis bending.
iii) To perform a statistical analysis for examining the existing expressions for effective flexural stiffness in the ACI code.
iv) To develop a nonlinear *EI* equation for calculating the flexural stiffness of partially encased composite columns subjected to major axis bending.

The effective flexural stiffness (*EI*) for slender PEC columns will be evaluated using the slender column strength curve and the cross-sectional strength curve. Newmark's iterative procedure will be implemented to evaluate the second-order deflection of slender columns which will eventually be used to calculate the second-order moment for slender columns. Strain-compatibility and force equilibrium equations will be used to construct the cross-sectional strength curve, i.e. load moment interaction diagram for short columns. Finally, theory of elasticity will be implemented to calculate the effective flexural stiffness of the slender PEC column.

In order to examine the influence of several geometric and material parameters on the effective flexural stiffness (*EI*) of slender PEC columns, about 1200 isolated PEC columns will be selected. Each column will have different combinations of geometric and material properties. The geometric properties that can greatly affect the behaviour of PEC columns include the column cross-sectional dimensions, length of the column, longitudinal spacing of the transverse links, thickness of the steel flange and web plates,

and initial load eccentricity. The compressive strength of concrete and yield strength of steel plates are considered as the material variables. The geometric properties listed here will be non-dimensionalised for comparison in order to reflect anticipated combined influences. The columns will be bent about the major axis of the encased steel section in symmetrical single curvature bending in braced frames subjected to short term loads.

1.3 ORGANIZATION OF THE THESIS

The thesis consists of five chapters. Chapter 1 introduces the type of composite column studied herein and presents the objectives and scope of the research work.

Chapter 2 presents a short review on the literature related to PEC columns with standard steel sections and explores in relative detail of the experimental and numerical research works carried out on PEC columns with thin-walled built-up steel sections. The previous research works in connection with effective flexural stiffness *EI* for fully encased composite columns are also presented in this chapter.

Chapter 3 includes the description of methodology for determining *P-M* (load-moment) interaction curves for PEC columns allowed to bend in a single curvature along major axis under eccentric loading. This chapter also describes the numerical procedures to develop a technique to determine the interaction curves including the secondary effects resulting from slenderness of the columns.

Chapter 4 describes the different parameters and their specified values for which PEC columns of a selected cross section are studied. Discussion on the effects of these different parameters on the PEC column is also presented in detail in this chapter.

In Chapter 5 a statistical analysis is performed on the calculated flexural stiffness of PEC columns covering a wide range of geometric and material parameters. The effective flexural stiffness for slender PEC columns obtained from this study is compared to the value obtained from the ACI (2005) code. A nonlinear equation for predicting the flexural stiffness is also presented in this chapter.

Finally, a brief summary of the study followed by conclusions and recommendations for future research are included in Chapter 6.

Chapter 2

LITERATURE REVIEW

2.1 INTRODUCTION

A PEC column section is an H–shaped steel section with concrete infill between the flanges of the section. In the early 1980s, PEC columns and beams were first introduced using standard-sized rolled steel sections in Europe. In 1996, the Canam Group in North America proposed a PEC column section constructed from a thin walled built–up steel H shape with transverse links provided at regular intervals to restrain local buckling. Using a built–up steel section instead of a standard shape provides the designer with more flexibility when sizing the column cross-section. To understand the behavior of PEC columns, on which the current study is being conducted, a review of the experimental and analytical investigations related to this composite system is presented in this chapter. This chapter also includes the capacity prediction models for calculating the axial and bending capacity of these columns. A brief discussion on the research conducted of effective flexural stiffness *EI* for slender columns are also incorporated.

2.2 PEC COLUMNS FABRICATED WITH STANDARD SECTIONS

Several experimental investigations (as described below) have been carried out on PEC beam-columns with fabricated shapes, typically used in Europe, subjected to static, cyclic and earthquake loading. The conventional form of this composite column consists of a compact steel section with longitudinal and tie reinforcements in the encased concrete.

2.2.1 Hunaiti and Fattah (1994)

Hunaiti and Fattah (1994) tested nineteen PEC columns under monotonic eccentric axial loading. The columns, which were made with slandered steel shape, were

divided into two groups. The purpose of the first group was to determine if PEC columns would act compositely without additional shear connectors. The purpose of the second group was to determine the behaviour of PEC columns fabricated with either shear connectors or batten plates at various load eccentricities. All columns were fabricated from IPE 200×100×22 steel sections (German standard size) and had an effective length of 2.4 m. The flange width-to-thickness ratio (*b*/*t*) for all specimens was 5.9. Of the ten PEC columns of the first group, five were made with low strength concrete (9.7 MPa) and five were made with normal strength concrete (32.5 MPa). The load eccentricity at one end of the column was 70 mm and the eccentricity at the other end varied among tests. For all ten tests, the researchers observed that there were no signs of local buckling of the steel flanges or any distortion of the cross-section. Therefore, Hunaiti and Fattah (1994) concluded that the columns were able to develop the full flexural strength of the standard section and that full composite behaviour was achieved.

The second group consisted of nine PEC columns. Of these, three had shear studs welded along the centerline of the web, three had 190mm×20mm×3mm steel batten plates welded between the tips of opposing flanges on both sides, and the remaining three had no additional steel added. All were cast with 51 MPa concrete. Each column type was tested at eccentricities of 30 mm, 50 mm, and 70 mm. For each eccentricity, the columns had similar column strength, regardless of whether additional steel was used. From these results, Hunaiti and Fattah (1994) concluded no additional steel was required to achieve full composite behaviour between the infill concrete and the steel section. However, the researchers recommended the use of mechanical shear connectors in design because the concrete in real structures is affected by factors that are not present in a laboratory setting, such as deceased bond between the steel and the concrete as the concrete ages.

2.2.2 Elnashai and Broderick (1994)

Elnashai and Broderick (1994) tested four PEC columns under cyclic and pseudo-dynamic loading. All were fabricated with 845 mm long, 152× 152×23 UC steel sections (British standard size) and infilled with 28 MPa concrete. The *b/t* ratio for the steel flanges was 11.2. Before casting the columns, 6 mm diameter steel rods were

welded between opposing flanges on both sides of the column to act as transverse links and provide increased confinement for the concrete. The rods used by Elnashai and Broderick (1994) were similar to the battens used by Hunaiti and Fattah (1994) except that the rods were welded 10 mm in from the flange tip while the battens were welded at the flange tip. The column behaviour under these loading conditions was compared to previous tests by Elnashai *et al.* (1991) wherein the columns had four 10mm diameter longitudinal reinforcing bars tied with 6 mm diameter stirrups in addition to the transverse links. The researchers concluded that the capacity of the PEC columns with only the transverse links was marginally less than the PEC columns with the additional reinforcing bars. However, they stated that the fabrication cost savings of the link-only PEC columns significantly offset the minor capacity loss and made the link-only PEC columns a more attractive alternative.

2.2.3 Plumier *et al.* (1995)

Plumier *et al.* (1995) tested 12 full-sized test specimens that consisted of a PEC column connected to a PEC beam. The specimens were tested under cyclic loading to examine primarily the behaviour of the joint region. The PEC beams were constructed from 1500 mm long (from the working point in the joint) HE 260 A steel sections (European standard size) that were infilled with 53 MPa concrete. The beam sections were modified by welding 6 mm diameter transverse links 30 mm from the flange tips. The links were spaced at a 150 mm. Two additional 6 mm diameter longitudinal bars were also added at mid-depth. The PEC columns were constructed from 3000mm long (between inflection points above and below the joint) HE 300 B steel sections that were also infilled with 53 MPa concrete. Similar to the PEC beams, the PEC columns were modified with transverse links and additional longitudinal bars. The *b/t* ratios for the PEC beams and columns were 10.4 and 14.3, respectively. Two fixed-connection types were used to attach the beams to the columns: bolted and welded. For each connection type, they used three different web thicknesses and two different cyclic testing procedures (total of six specimens per connection type). From these tests, Plumier *et al.* (1995) observed that neither the connection type nor the web thickness affected the performance of the specimen. Furthermore, they noted that all

yielding took place in the beams and that the beam flanges always buckled outward due to the presence of the concrete.

2.3 EXPERIMENTAL INVESTIGATIONS AND CAPACITY PREDICTION MODELS FOR SHORT THIN WALLED PEC COLUMNS

Extensive experimental research has been conducted on thin-walled PEC columns with built–up sections by several research groups (Fillion 1998; Tremblay et al. 1998; Chicoine *et al.* 2000, 2002a, 2002b, 2003; Muise 2000; Bouchereau and Toupin 2003; Prickett and Driver 2006) to investigate the behaviour of this type of PEC column under various loading conditions. Capacity prediction models for these columns under concentric and eccentric loads have also been developed by Tremblay et al. 1998; Chicoine *et al.* 2000 and Prickett and Driver 2006.

2.3.1 Tremblay *et al.* (1998)

In 1996, collaboration between the Canam Group Inc. and Ecole Polytechnique de Montreal resulted in a new design concept for a partially encased composite (PEC). The Canam type of PEC column is significantly different from previous research because the steel section was fabricated from relatively thin plates to make the section lighter than standard sections. However, the thin plates are more susceptible to local buckling. Therefore, transverse links, similar to those used by Elnashai and Broderick (1994), were required to prevent local buckling of the bare steel shape.

For the initial phase of the research program, six PEC stub columns (Figure 2.1) were tested and analyzed by Tremblay *et al.* (1998). Each column had a square cross-section (either 300mm×300mm or 450mm×450 mm) and a length that was five times the cross-sectional dimension. As well, each column was fabricated with CSA-G40.21-350W grade steel and was cast with normal strength concrete (ranging from 32 to 34 MPa). The main parameters examined were the spacing of the links (ranging from half of the cross-section depth to the full cross-section depth), the flange *b/t* ratio (ranging from 23 to 35), and the overall size of the columns (as noted above). The *b/t* ratio for this type of PEC column was much higher than that for PEC columns fabricated from standard shapes (ranging from 6 to 14) making it more susceptible to local buckling.

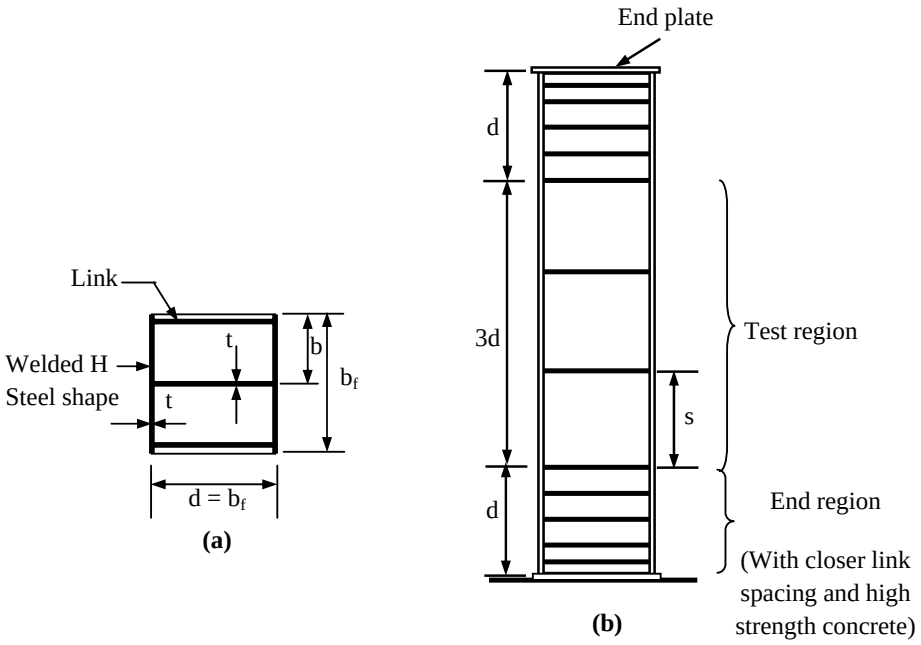

Figure 2.1: Typical PEC Test Column, (a) Cross-section, (b) Elevation

In addition to the composite columns, ten bare steel specimens of similar dimensions were tested to determine the capacity with a variety of steel shapes (including smooth rod, deformed bar, and steel plate) used as transverse links (Filion 1998). The capacity of the bare steel section was calculated using Canadian standard CSA S 136-94 (CSA 1994), which uses a reduced effective cross-sectional area in calculating the capacity of members susceptible to local buckling. The mean test-to-predicted ratio of the bare steel columns was 1.22 (Filion 1998), with a low value of 0.95. The high test-to-predicted ratio indicates that the design capacity of the bare steel shape is generally conservative regardless of what steel shape was used as the transverse link.

The failure mechanism was similar for all of the composite columns in this study. Failure occurred by crushing of the concrete combined with local buckling of the steel flange near the crushed concrete as shown in Figure 2.2. Tremblay *et al.* (1998) observed that columns having larger link spacing exhibited a faster degradation of post-peak strength than columns with smaller link spacing. The researchers concluded that a smaller link spacing result in a more ductile response. The column with the largest width-to-thickness (*b/t*) ratio had a lower strength than similar columns with stockier flanges and exhibited a sharper drop in post-peak strength.

Tremblay *et al.* (1998) developed a mathematical model to predict the strength of the PEC stub columns. The model calculates the contribution from the steel and the concrete separately and then adds them to predict the overall column strength,

$$C_r = 0.85A_c\, f_c' + A_{se}F_y \qquad \ldots (2.1)$$

In Equation (2.1), 0.85 is a factor that relates concrete cylinder strength to in-situ concrete strength, A_c is the cross-sectional area of concrete, f'_c is the concrete cylinder strength, and F_y is the yield strength of the steel. The thin-walled steel section is susceptible to local buckling, so its full cross-sectional area is reduced to an effective steel area, A_{se} using the effective width method based on von Karman's formula,

$$A_{se} = t(d-2t-2b_e) \qquad \ldots (2.2)$$

Where,

$$b_e = \alpha \frac{b}{\lambda_p} \leq 1 \qquad \ldots (2.3)$$

$$\lambda_p = \frac{b}{t}\sqrt{\frac{12\left(1-\nu_s^{\,2}\right)F_y}{\pi^2 E_s k}} \qquad \ldots (2.4)$$

$$k = \frac{4}{\left(s/b_f\right)^2} + \frac{15}{\pi^4}\, s/b + \frac{20}{3\pi^2}(2-3\nu) \qquad \ldots (2.5)$$

In Equation (2.2), t is the thickness of the steel plate, d is the depth of the cross-section, and b_e is the effective half-flange width as calculated using Equation (2.3). In Equation (2.3), α is an empirical factor to account for initial imperfections and residual stresses taken by Tremblay *et al.* (1998) as 0.6, λ_p is a slenderness parameter for the flanges as calculated in Equation (2.4), and b is the actual half-flange width. In Equation (2.4), ν and E are Poisson's ratio and Young's modulus for steel. Also in Equation (2.4), k is the plate buckling coefficient calculated using Equation (2.5), wherein s is the centre-to-centre link spacing. Equation (2.5) was developed

from energy methods that assumed that the flanges buckled outward between adjacent links.

The use of this model (Equations 2.1 to 2.5) produced results that predicted the test results within 3%. Tremblay *et al.* (1998) recommended that larger specimens be tested to determine if size variations affected the validity of their model.

2.3.2 Chicoine *et al.* (2002a)

As an extension of the research presented by Tremblay *et al.* (1998), Chicoine *et al.* (2002a) tested five PEC stub columns measuring 600mm×600mm×3000mm to determine if size effects were present in the model presented in the earlier work. The columns had 16mm diameter links, spaced at either 300 mm or 600 mm, and were cast with 34 MPa concrete. Chicoine *et al.* (2002a) also studied the effects of additional reinforcement by including reinforcing bars and stirrups in one of the five specimens. As well, the transverse stresses in the steel section and the links due to the lateral expansion of the concrete were recorded to determine if they reduced the capacity of the steel section.

The bare steel section was studied to determine the shape and extent of local imperfections between the links. Due to the fabrication process, shrinkage of the welds between the web and flanges tends to cause the flanges to bend inward before the links (with a length consistent with the nominal column dimension) are inserted between them and welded in place. Thus, the flanges tend to have a slight residual inward bow between adjacent links. Chicoine *et al.* (2002a) determined that the local imperfections were more pronounced when the link spacing was larger. Furthermore, comparing with previously tested specimens, they concluded that the local imperfections, when normalized by link spacing, were less on larger specimens. Chicoine *et al.* (2002a) speculated that the slight inward imperfections benefit the local buckling resistance of the steel flange after the concrete has been placed.

The failure mechanism observed by Chicoine *et al.* (2002a) was consistent with previous tests; the concrete crushed as the steel flanges buckled (Figure 2.2).

Nevertheless, it was noted that local buckling began at 75% of the peak load in specimens where the link spacing was equal to the column depth *d*.

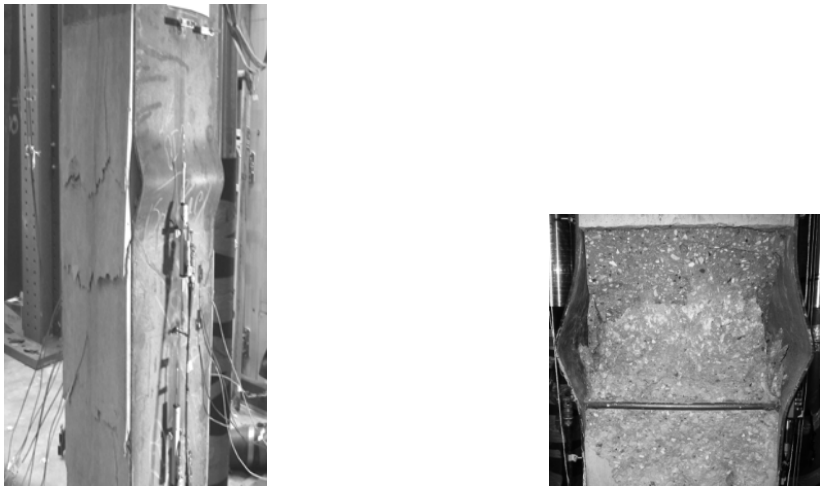

Figure 2.2: Failure Mode of Typical PEC Test Column (Chicoine et al. 2002).

For the columns with link spacings equal to 0.5*d*, the flanges did not buckle until the peak load and the PEC column underwent a more ductile failure. From these observations, Chicoine *et al.* (2002a) recommended that PEC columns be designed with a link spacing of 0.5*d*.

The longitudinal and transverse stresses in the steel plate were calculated from strain measurements by assuming a bi-axial stress state. The von Miser stress was also calculated. For all five columns, the transverse stress was found to be negligible and the longitudinal stress to be similar to the von Mires stress until the peak load was reached. Therefore, the researchers concluded that the lateral expansion of the concrete did not induce significant transverse stress in the steel section. Thus, the axial capacity of the column is unaffected by the lateral expansion of the concrete.

The columns with links spaced at 0.5d experienced higher stresses (296 to 303 MPa) than the columns with links spaced at *d* (90 to 151 MPa). Chicoine *et al.* (2002a) concluded that the higher stresses were due to the increased confinement of the

concrete provided by the closer spaced bars. Also, they noted that the increase in link stresses was nearly proportional to the decrease in link spacing. From their results, two conclusions were reached. First, the cross-sectional area of the link should be the greater of (i) 0.025 times the column depth d times the plate thickness t; or (ii) $100mm^2$. Second, the weld connecting the link to the flanges should be designed such that the link can develop its full yield strength.

The capacity prediction model by Tremblay *et al.* (1998) was found to be less accurate for the 600mm×600mm columns than for the smaller specimens tested in the previous research. Therefore, Chicoine *et al.* (2002a) proposed two significant modifications to the design equations of Tremblay *et al.* (1998). First, in another paper by the same authors (Tremblay *et al.* 2000b), it was proposed that Equation (2.3) be replaced by Equation (2.6) with n being taken as 1.0 because it resulted in a better fit for the expanded test data set:

$$b_e = b(1+\lambda_p^{2n})^{(-1/n)} \qquad \ldots(2.6)$$

Second, the 0.85 term in Equation (2.1) was replaced by the variable Ψ, which accounts for the concrete size effects on the cross-section strength:

$$\psi = 0.85\left(0.96 + \frac{22}{b}\right)\left(0.85 \le \psi \le 0.97\right) \qquad \ldots(2.7)$$

Equation (2.1) was therefore rewritten, also including an additional term to account for the possible presence of longitudinal reinforcement as,

$$C_r = \psi A_c f'_c + A_{se} F_y + A_r F_{yr} \qquad \ldots(2.8)$$

Where A_r and F_{yr} are the cross-sectional area and yield strength of the reinforcing bars, respectively.

2.3.3 Bouchereau and Toupin (2003)

Bouchereau and Toupin (2003) tested 22 PEC columns and two PEC beams to determine their behaviour in bending and under cyclic loading. All 22 columns were of dimension 450mm×450mm×2250mm, with 16mm diameter links spaced at 300mm (0.67*d*). The two beams were of dimension 450mm×450 mm×5000mm, with 16mm diameter links spaced at 300 mm. All 24 specimens were fabricated with CSA-G40.21-35OW grade steel plate and 34 MPa concrete. The plate thickness for all 24 specimens was 9.53 mm, resulting in a flange width-to-thickness ratio of 23.6. Eleven columns and one beam had four additional 20M reinforcing bars tied with 10M stirrups. Thirteen static tests were performed, including six specimens with additional steel reinforcement, and 11 cyclic tests were performed, including six specimens with additional steel reinforcement. The cyclic loading pattern contained a combination of both large and small amplitude cycles.

Bouchereau and Toupin (2003) compared the results from cyclic tests with the results from companion static tests. They concluded that a PEC column had similar capacity whether the column was tested cyclically or statically. Furthermore, there was no significant difference in post-peak strength between columns tested cyclically or statically.

The use of additional steel bar reinforcement confirmed the previous findings that it increased the ductility of the column with a marginal increase in ultimate column strength. Bouchereau and Toupin (2003) noted that their specimens failed in a ductile manner when subjected to cyclic loading, regardless of the presence of additional steel reinforcement.

The column test results were compared to column interaction diagrams constructed by assuming a linear strain distribution across the cross-section. The strain at one extreme fiber was set to the concrete crushing strain and the strain at the other extreme fiber was varied to establish points on the diagram in a manner similar to that generally used for deriving interaction diagrams for reinforced concrete columns. A crushing strain of 3500με was assumed for the concrete. The model neglected local

imperfections and local buckling of the steel section. Despite these omissions, the test results fit reasonably well on the PEC column interaction diagram

Bouchereau and Toupin (2003) recommended that the PEC column interaction curves could be improved by considering local buckling of the flanges, residual stresses in the steel section, and confinement of the concrete, although it would increase the complexity in producing the interaction diagrams.

2.3.4 Prickett and Driver (2006)

Prickett and Driver (2006) conducted a comprehensive experimental research project to study the behaviour of thin-walled PEC columns made with high performance concrete. The study included 11 short PEC columns measuring 400mm×400mm×2000mm, with the primary variables being the concrete type, link spacing and load eccentricity. The plate slenderness ratio was kept constant (b/t = 25) for all of the test columns.

The specimens were divided into two groups. The first group consisted of seven specimens subjected to axial compression only. Three different link spacings and three types of concrete (normal strength, high strength and high strength steel fiber reinforced concrete) were used in these specimens. Two normal strength concrete columns with different link spacings were used as reference specimens. Steel fibers were used to observe potential improvement in the failure mode of PEC columns with high strength concrete. In the second group of specimens, four identical PEC columns constructed with high strength concrete and subjected to axial compression and bending were tested by Prickett and Driver (2006). Bending axis and the amount of load eccentricity were varied to determine the effects of these parameters on the column behaviour. Initial local imperfections in the flange plate were measured at several locations in the steel section for all 11 test specimens. The local imperfections in the flanges were observed to be inwards in most locations, with average maximum amplitude of approximately 1.5mm (s/375). Additional measurements of the local flange imperfections were performed after the columns had been cast and no significant differences were observed.

The column behaviour was examined by considering the failure mode, load versus strain response and the transverse stresses in the steel plates. The high strength concrete PEC columns failed in a similar manner to the PEC columns with normal strength concrete, concrete crushing combined with local flange buckling. However, the failure of a high strength concrete column was observed to be sudden as compared to an equivalent PEC column with normal strength concrete. Addition of steel fibers in the high strength concrete was found to improve the failure mode of the columns somewhat. Prickett and Driver (2006) reported no local buckling prior to the peak load in any of the concentrically loaded test specimens, even for the specimen with a link spacing equal to the depth of the column However, one of the eccentrically loaded specimens experienced local buckling at 90% of the peak load. The effect of confinement, as revealed by transverse stresses in the steel section, on the capacity of the high strength concrete PEC columns was similar to that observed for the normal strength concrete PEC columns. However, the steel section of columns with high strength concrete yielded sooner relative to the peak load as compared to the steel section of the column with normal strength concrete. The axial capacity of the high strength concrete PEC columns was not significantly affected by the confinement of the concrete and therefore Prickett and Driver (2006) recommend that confinement not be accounted for in the design of these columns. The maximum stresses in the links were well below the yield stress and therefore it was recommended by the researchers that the current design requirements for link cross-sectional area and welding in CSA standard S16-01 (CSA 2001) are satisfactory for high strength concrete PEC columns under concentric and eccentric loading conditions.

Prickett and Driver (2006) also studied the moment versus curvature response and developed load versus moment interaction diagrams for the eccentrically loaded specimens. The moment versus curvature curves for specimens with strong axis bending showed a gradual decline of the peak moment as compared to the sudden decline observed in the specimens with weak axis bending. To predict the capacity of the eccentrically loaded columns, the load versus moment interaction diagrams were developed using the methods used for reinforced concrete columns. However, Prickett and Driver (2006) used the reduced steel area in calculating the design

capacity to account for the local buckling of the flanges, since local buckling was observed in a few eccentrically loaded columns shortly before the peak load. A linear strain distribution along the cross-section, based on observations from the strain measurements taken during the test, was implemented for the construction of this diagram. The extreme compressive strain was set at 3500 με (considered to be the crushing strain of concrete), whereas the extreme tensile strain was varied from 0 to 10 times the yield strain of the steel. For each strain gradient the ultimate load and moment capacities were calculated from the material and geometric properties of the composite cross-section. The compressive force in the concrete, C_c was calculated using the following expression, assuming a rectangular stress block:

$$C_c = \alpha_1 f_{cu} b_c \beta_1 c \qquad \ldots\ldots (2.9)$$

where b_c is the net width of the concrete block (i.e., excluding the web thickness for strong axis bending and excluding the flanges for weak axis bending), c is the distance between the extreme compression fiber and the neutral axis and the factors α_1 and β_1 are expressed as (CSA 2004),

$$\alpha_1 = 0.85\text{-}0.0015\, f_{cu} \geq 0.67 \qquad \ldots (2.10)$$

$$\beta_1 = 0.97 - 0.0025 f_{cu} \geq 0.67 \qquad \ldots (2.11)$$

To calculate the contribution of the steel to the capacity of the composite column, the section was discretised in such a way as to have effectively uniform strain in each individual piece. For strong axis bending, the flanges were considered to be one piece, whereas the web was divided into ten pieces. On the other hand, for weak axis bending the web was considered as one piece and each flange was discretised into ten pieces (Prickett and Driver 2006). The resultant force for each individual piece was calculated by multiplying the area of the piece by its average strain and by the elastic modulus of steel. (However, if the strain in the individual piece exceeded the yield strain the force resultant is determined by multiplying the area of that piece by the yield stress.) In calculating the area of a flange piece in compression, the effective width (using Equation 2.6 with n = 1.5) was used by Prickett and Driver (2006). Finally, the total load capacity of the composite column was determined by adding

the force resultants for concrete and steel and the moment capacity were obtained from the summation of each force multiplied by its distance from the centerline of the column cross-section.

In general, the interaction curves provided a good and conservative estimate of the ultimate cross-sectional capacities of the eccentrically loaded PEC columns obtained from the tests. For columns with strong axis bending, the capacities obtained from the test exceeded the predicted capacities by 17 to 27%, whereas for columns with weak axis bending the predicted capacities were exceeded by only 4 to 9%. Prickett and Driver (2006) attributed this discrepancy to the fact that the concrete confinement, which was neglected in predicting the column capacities, had a more pronounced effect on the columns under strong axis bending than on those under weak axis bending. The presence of a steel flange on the face that experiences maximum compression provides more favorable confinement conditions than either columns under weak axis bending or those loaded concentrically.

2.4 NUMERICAL INVESTIGATIONS ON SHORT PEC COLUMNS

Numerical investigations performed to study the behaviour of PEC columns are limited. Maranda (1998), Chicoine *et al.* (2002b) and Begum *et al.* (2007) conducted numerical simulations of the behaviours of PEC columns under concentric and eccentric axial loads. A brief description and findings of these simulations are presented below.

2.4.1 Maranda (1998)

A finite element model of PEC columns with thin–walled built–up sections was first developed by Maranda, (1998), using the computer program MEF, to simulate the series of tests on PEC stub columns performed by Tremblay *et al.* (1998). Only a quarter cross–section was modeled using shell elements for the steel plate, solid elements for the concrete and beam elements for the transverse links. Contact elements were used at the steel–concrete interface to represent interaction between these two materials. The model included local imperfections of the steel flange by scaling the displacements obtained from the buckled elastic shape. The yield plateau

of the steel stress–strain curve was modified to include the effect of residual stresses in the steel plates. Good agreement was observed between the numerical and the experimental results, with an average ratio of experimental-to-numerical peak loads of 0.95 and a standard deviation of 0.03. However, the model developed by Maranda (1998) was not capable of predicting the post-peak responses of the test specimens. In some cases the model exhibited positive stiffness at the last converged solution point, indicating that the ultimate point had not been reached. Moreover, local imperfections were modeled outwards as opposed to the inward imperfections measured in the test specimens.

2.4.2 Chicoine *et al.* (2002b)

Following their own recommendations, Chicoine *et al.* (2002b) developed a finite element model that agreed with existing test data and that could be used to predict the long term behaviour of PEC columns. Three changes to the existing design equations were recommended in this work. First, to better fit the experimental data, the factor T was reduced by a factor of 0.92. Second, the value of $n = 1.0$ in equation (2.6) may be overly conservative. By adding the long-term tests to the database collected by Tremblay *et al.* (2000), Chicoine *et al.* (2002b) calculated a mean test-to-predicted ratio of 1.00 when $n = 2.0$ and a ratio of 1.03 when $n = 1.5$. Considering that larger imperfections than those measured on the test specimens would be acceptable under the fabrication tolerances of the Canadian steel design standard (CSA 2001), the researchers recommended that $n = 1.5$ be used. Third, the plate stiffness coefficient, k (Equation 2.5), was modified based on the results of elastic finite element buckling analyses of steel column flanges. Its new form, presented in Equation (2.12), assumes a Poisson's ratio of 0.3 in the constants.

$$k = \frac{3.6}{\left(s/b\right)^2} + 0.05\left(s/b\right)^2 + 0.75, \left(1 \le s/b \le 2\right) \qquad \ldots(2.12)$$

It was also noted that their model predicted that the long-term effects on the column due to the shrinkage and creep of the concrete would not adversely affect the axial capacity of the column.

Chicoine *et al.* (2002b) found that, while their model accurately predicted column capacity and strain at peak load, the failure mode could only be predicted properly by implementing initial outward flange imperfections rather than inward, as observed in the test specimens. This was attributed to the inability of the model to reproduce the rapid volumetric expansion of the concrete near peak loading. For the same reason, the model could not trace the post-peak behaviour of the columns.

2.4.3 Begum *et al.* (2007)

To improve the numerical model of PEC columns produced by Chicoine *et al.* (2002b), Begum *et al.* used a damage plasticity model to simulate the concrete behaviour and a dynamic explicit solution strategy. The researchers postulated that the material model would improve the results around the peak load because it is capable of predicting volumetric expansion under low confining pressures. Moreover, the dynamic explicit method has the potential to predict results in the range beyond the peak load. The stub column test results from Tremblay *et al.* (1998) and Chicoine *et al.* (2002a) were compared to numerical model. The mean experimental-to-numerical ratio for the column peak load and longitudinal strain at peak load were 1.00 and 0.98, respectively. The model also gave good agreement with the post-peak response and the failure mode observed during testing.

A complete finite element model including the full cross-section and entire length of the column was developed using the explicit module of ABAQUS finite element code (Begum *et al.* 2007). The model is applicable for concentric as well as eccentric loads. The finite element model along with the mesh configuration for a typical part between two consecutive links is shown in Figure 2.2. The steel plates were modeled using S4R shell elements. Eight-node brick elements were used for concrete and beam elements for transverse links. A dynamic explicit solution strategy was implemented in to trace a stable post peak response in the load–deformation curve. The steel–concrete interface in the composite column was simulated using a contact pair algorithm. To represent the concrete material behaviour under partial confinement, the damage plasticity model in ABAQUS was implemented.

Begum et al. (2007) used the complete model for PEC columns to reproduce the test results of 12 normal strength, seven high strength and two steel fiber-reinforced high strength concrete PEC columns. The average experimental-to-numerical ratios of the

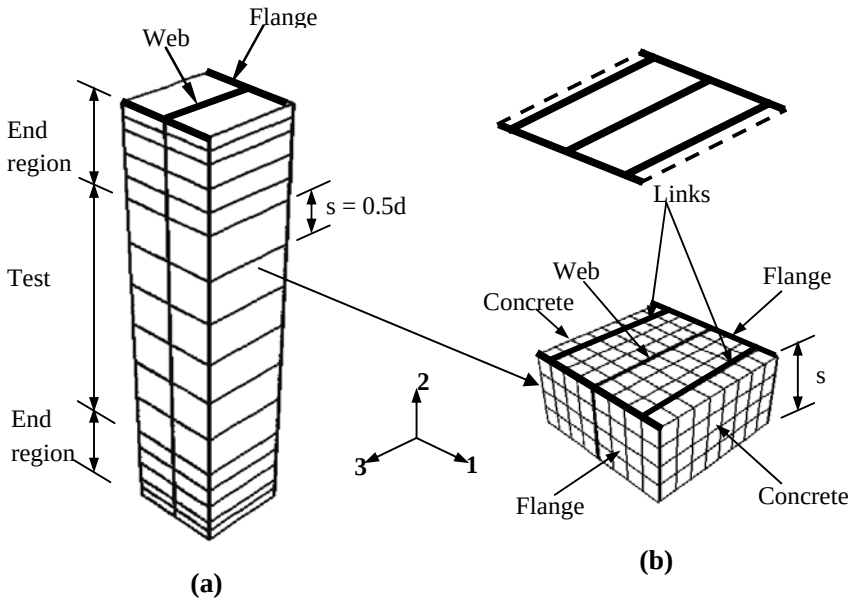

Figure 2.3: Finite Element Mesh developed by Begum et al.(2007),
(a) Typical short column displaying the parts between consecutive links, and
(b) Mesh configuration of a typical part in the test region of the column

peak load obtained were: 1.01, 0.99 and 1.08, respectively, for normal strength, high strength and steel fiber reinforced high strength concrete PEC columns with standard deviations all less than 0.05. Moreover, the numerical load versus axial strain responses for the test columns were in very good agreement with the experimental responses. Furthermore, the load versus moment curves obtained from the numerical analyses of the eccentrically loaded test columns represented the experimental curves with excellent accuracy, for strong axis bending as well as weak axis bending. The full model also represented the axial capacity of the three long PEC test specimens (L/d = 20) with good accuracy with an average experimental-to-numerical ratio of 0.98.

Studies were performed to quantify the effects of local imperfections and residual stresses on the capacity of these columns using the developed model. The results revealed that the ultimate capacity of the column was not affected significantly by the presence of local imperfections and residual stresses in the steel section (Begum *et al.* 2007). Finally, a comprehensive parametric study was carried out by varying the overall column slenderness ratio, load eccentricity, link spacing, slenderness ratio of the steel plate and concrete strength to explore the behaviour of these columns under the combined effect of axial compression and bending about the strong axis.

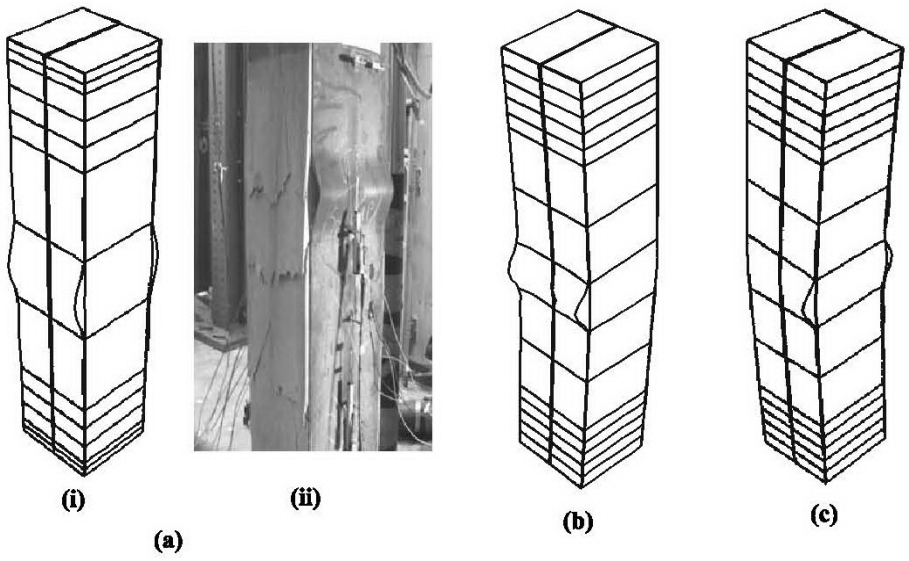

Figure 2.4: Failure modes obtained from the full column FE model for short PEC columns developed by Begum et al.(2007),
(a) Concentric load, (i) Numerical & (ii) Experimental (Prickete & Driver2006)
(b) Eccentric load (strong axis bending)
(c) Eccentric load (weak axis bending)

2.5 INVESTIGATIONS ON THE BEHAVIOUR OF SLENDER PEC COLUMNS

Experimental and numerical investigations on slender PEC columns are very limited. The only experimental investigation has been performed at Leheigh University by Chicoine *et al*. (2000) and numerical simulations of these test specimens are

conducted by Begum *et al.* (2007). Begum *et al.* (2007) also conducted a parametric study to observe the effect of several geometric variables on slender PEC columns.

2.5.1 Experimental study by Chicoine *et al.* (2000)

Chicoine *et al.*(2000) tested four long PEC columns with a length-to-depth ratio of 20 in order to study the overall buckling behaviour of these columns under monotonic loading. In this test program, one bare steel column and three composite columns were tested with two different link spacings. All columns had a square cross-section of 450mm×450mm and a flange slenderness ratio of 23. Additional longitudinal and tie reinforcements were provided in one of the composite specimens. Both local and global geometric imperfections were measured in all specimens before the tests took place. The flanges of these specimens were observed to have outward local imperfections between links, with maximum amplitudes less than 1 mm (*s*/600). The global out-of-straightness was measured about the weak axis and was also found to be small, representing typically about 1/3000 of the total height of the columns. The long columns were tested under concentric loading, except for one, which was tested with an eccentricity of 0.06*d* about the weak axis. However, Chicoine *et al.* (2000) reported the presence of significant bending moment in all specimens about both the strong and weak axes caused by accidental eccentricity or uneven end bearing. Equivalent strong and weak axis eccentricities were, therefore, calculated for each specimen at the bottom, mid-height and top elevations using elastic theory. Chicoine *et al.* (2000) recommended that these computed values of eccentricity be included in the finite element analysis of these test specimens.

The test results demonstrated the brittle and explosive failure modes of the long composite specimens that consisted of global flexural buckling along with local buckling and concrete crushing between two links. The steel-only specimen was observed to fail by global buckling followed by local buckling at several link intervals. As reported by Chicoine *et al.* (2000), no welds of the transverse links failed during the tests. The ultimate capacities of the slender columns were observed to be about 80% of those of short columns with similar cross—sections and link spacings. The initial weak axis eccentricity of 0.06*d* applied in one of the tests

decreased the column capacity by 20% when compared with the specimen having similar geometric and material properties. The transverse stresses on the flange plates were observed to be higher on the compression side and lower on the tension side, with intermediate values in the web. The additional reinforcement was observed to provide no improvement in the ductility of the long composite column, as opposed to the beneficial effect observed in the short composite columns. However, a direct comparison between the two long specimens with and without additional reinforcements was not possible due to the presence of accidental eccentricity in the test specimens.

Chicoine *et al.* (2000) predicted load capacity for this column. The double exponential format is similar to other slender column capacity calculations found in CSA S16-01 (CSA 2001).

$$C_u = C_r\left(1+\lambda^{2.68}\right)^{-1/1.34} \qquad \ldots (2.13)$$

$$\lambda = \sqrt{\frac{C_r}{C_{ec}}} \qquad \ldots (2.14)$$

$$C_{ec} = \frac{\pi^2 EI_e}{(KL)^2} \qquad \ldots (2.15)$$

$$EI_e = EI_s + \frac{0.6E_cI_c}{1+D/T} \qquad \ldots (2.16)$$

For the further development of PEC columns, Chicoine *et al.* (2002a) recommend the testing of columns, in bending due to eccentric loading and the development of a validated finite element model.

2.5.2 Numerical Study by Begum *et al.* (2007)

Begum *et al.* selected three 9.0m long PEC columns with a cross–section of 450mm×450mm tested by Chicoine *et al.* (2000) and named CL-1, Cl-2 and CL-3 for finite element simulation with ABAQUS/Explicit in order to study the ability of the models to predict the global buckling behaviour. An elevation of a typical long PEC

test column is shown in Figure 2.4 a. Normal strength concrete was used in the test region of these columns.

In the test region of these columns, two types of links spacings were used: 1.0*d* in specimens CL-1 and CL-2, and 0.5*d* in specimen CL-3. Additional reinforcements were provided only in specimen CL-3 (Figure 2.4 c).

Among these three specimens, one (specimen CL-2) was intended to have eccentric loading, where the load was applied at an eccentricity of 28 mm, resulting in bending about the weak axis. These columns were also fabricated from CSA-G40.21-350W grade steel plate. Normal strength concrete (nominally 30 MPa) was used in the test region of these columns. To strengthen the end regions of these test specimens, high strength concrete of 60 MPa nominal strength was used along with the closer link spacings provided in these zones.

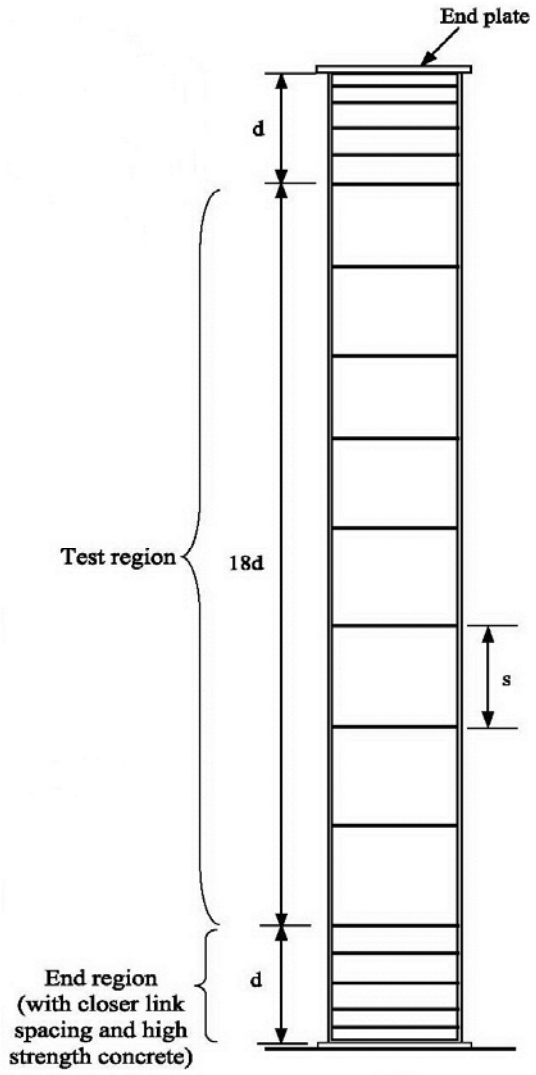

(a)

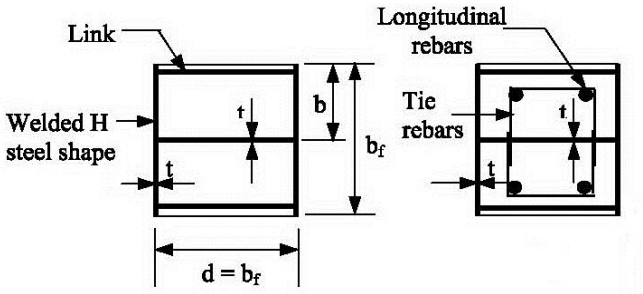

Figure 2.5: Long PEC test columns numerically simulated by Begum et al. (2007)
(a) Elevation, (b) Cross section of CL-1 & CL-2, (c) Cross section of CL-3

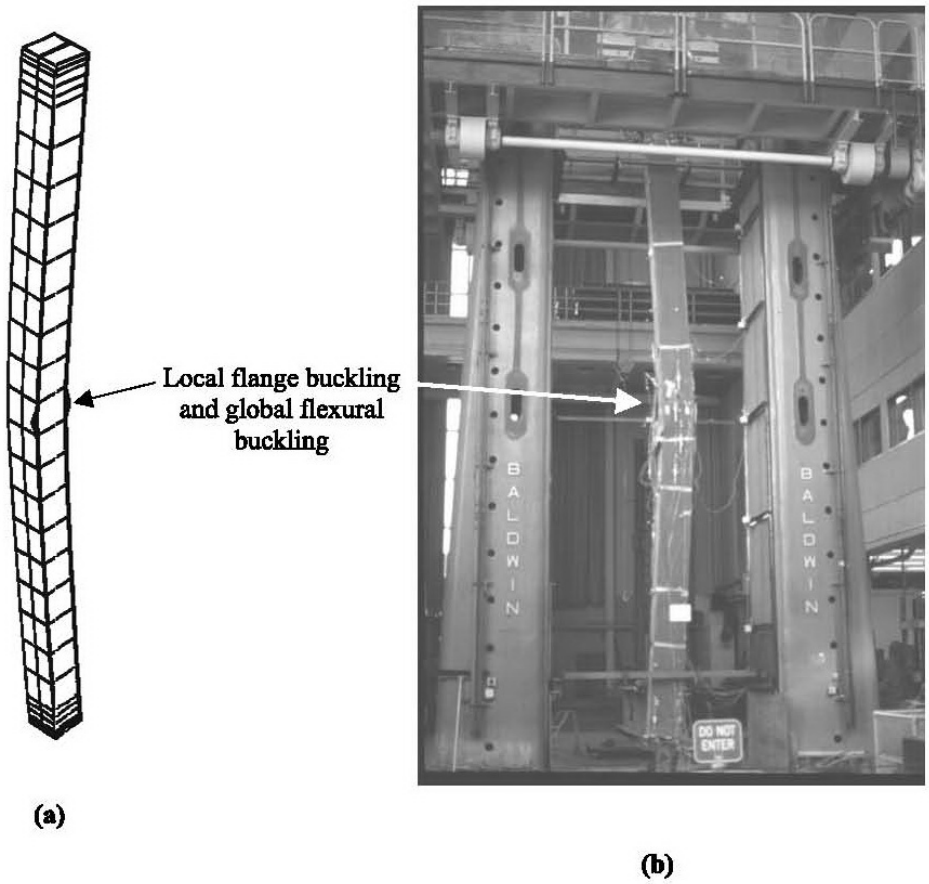

Figure 2.6: Numerical and Experimental failure modes for Long PEC columns
(a) Numerical failure (Begum et al. 2007) &
(b) Experimental failure (Chicoine et al. 2000)

Two sets of numerical analyses were performed for each of the long test columns, one using the applied eccentricity and the other using the eccentricities deduced from strains measured during the test. For specimens CL-1 and CL-2, the test load versus strain response was observed to be close to the numerical response using the deduced eccentricities. But for CL-3, neither of the two numerical analyses was observed to predict the experimental behaviour well, yet the response with the deduced eccentricities is much closer to the experimental response. However, for all three long columns, the numerical model gave an accurate prediction of the initial axial stiffness observed in the experimental load versus strain curve and the axial strains at and after

the peak load point were observed to be higher in the numerical models as compared to those obtained experimentally. The behaviour of the slender columns tends to be sensitive to loading and geometric imperfections present in the test.

In the numerical analysis of slender columns, failure occurred due to global bending of the column about the weak axis accompanied by local flange buckling and concrete crushing as shown in Figure 2.5(a). Similar behaviour was observed in the experiments performed by Chicoine *et al.* (2000).

2.6 INVESTIGATIONS ON FLEXURAL STIFFNESS OF SLENDER COMPOSITE COLUMNS

The flexural strength of a slender column subjected to end moments causing symmetrical single curvature bending is lower than the strength of its cross-section due to the second-order bending moment. The behavior of slender columns is greatly influenced by the critical buckling load, which again is dependent on the effective flexural stiffness of the slender column. The *EI* expressions given in ACI 318-02 (ACI 2005), for composite columns were mainly developed for reinforced concrete columns. Mirza and Tikka (1999) performed a statistical evaluation to judge the applicability of this equation for the flexural stiffness of composite columns in which steel shapes are fully encased in concrete.

Mirza and Tikka (1999, 2000) undertook extensive studies to examine the influence of a full range of variables on the short-term effective flexural stiffness (*EI*) of slender, tied, composite columns. In these studies the bending moment was applied about the major and minor axes of the steel sections fully encased in concrete. They also examined the existing expression for *EI* as proposed by American Concrete Institute (ACI) and Canadian Standards Association (CSA). They developed and proposed a refined expression for *EI* and compared the new expression for *EI* with the current ACI and CSA expression. Approximately 12,000 simulated isolated composite columns were used to generate the stiffness data to study the effects of a number of variables that affect the effective flexural stiffness. Each column had a

different combination of cross-section, geometric, and material properties. The specified concrete strength (f'_c), the structural steel yield strengths (F_y), the longitudinal steel reinforcing ratios (ρ_{rs}) and the structural steel ratios (ρ_{ss}) used in this study were intended to represent the most common values of these variables. All columns had reinforcing steel specified yield strength of 60,000psi (414MPa) with lateral ties conforming to ACI 318-95 clause 10.16.8. The slenderness ratios (*l/h*) selected were intended to approximate the range of *l/h* ratio for columns in braced frames designed according to ACI 318-95 clause 10.11 and 10.12. Eleven end eccentricity ratios (*e/h*) ranging from 0.05 to 1.0 were used. These end eccentricities produced bending moments about the major axis of the steel section. The usual *e/h* ratio for columns in concrete buildings varies from 0.1 to 0.65. The overall cross sectional dimensions were not varied because an earlier parametric study concluded that the gross cross section size had insignificant effect on non-dimensional strength and stiffness of composite columns.

The short term theoretical *EI* for each of the columns studied was computed from the following equation.

$$EI = \frac{P_u l^2}{4\left[\sec^{-1}\left(\frac{M_{cs}}{M_{col}}\right)\right]} \qquad \ldots (2.17)$$

In Eq. (2.17) *EI* is the theoretical effective flexural stiffness of a pin ended slender column subjected to single curvature bending with equal moments acting at both ends where M_{cs} and M_{col} are the flexural strength of cross section and flexural strength of the column taking the slenderness effect into account respectively for an ultimate axial load P_u. Finally the simulated column stiffness data were statically analyzed for examining the current ACI column stiffness equations and for developing the design equations for *EI* which is as follows:

$$EI = [(0.27 + 0.003l/h - 0.2e/h)E_c(I_g - I_{ss}) + 0.8E_s(I_{ss} + I_{rs})] \geq E_s I_{ss} \qquad \ldots(2.18)$$

$$EI = [(0.3 - 0.2e/h)E_c(I_g - I_{ss}) + 0.8E_s(I_{ss} + I_{rs})] \geq E_s I_{ss} \qquad \ldots(2.19)$$

2.7 CONCLUSIONS

The literature review shows that the behaviour of short Partially Encased Composite (PEC) columns with normal and high performance materials have become relatively well understood from the full scale experimental investigations for monotonic concentric and eccentric axial loading conditions. Extensive research has refined the design equation for concentrically-loaded PEC columns. The finite element models developed for this new composite system can adequately represent the local buckling behaviour, the ultimate load and the post-peak residual capacity for axial compression and bending. In addition, the influences of several key parameters, which could not be covered by the experimental programs, on the behaviour of these columns under axial compression and bending, were investigated using the finite element models. These studies are mainly confined to the exploration of the behavior of short PEC columns. Both experimental and numerical studies on the behaviour of long PEC columns are still very limited and no substantial study has yet been done on effective flexural stiffness (*EI*) of Partially Encased Composite columns in major or minor axis of steel section. Moreover, the influences of several key parameters on the slenderness behaviour of this kind of columns are yet to be investigated. Therefore, the existing guidelines in ACI and other codes to determine *EI* for thin walled PEC columns should be examined and extended, if needed, to cover the full range of variables affecting the behaviour of this type of composite columns.

Chapter 3

METHODOLOGY FOR EVALUATING THE THEORETICAL FLEXURAL STIFFNESS

3.1 INTRODUCTION

The American Concrete Institute building code ACI 318-08 (2008) permits the use of a moment magnifier approach for computing the second-order moments in slender composite columns. This approach was introduced into design practice to eliminate the need for extensive calculations which is based on the solution to a differential equation to compute second-order bending moments in columns. The calculation is also influenced by the critical buckling load (P_c). The computation of Euler's critical load P_c is strongly influenced by the effective flexural stiffness (EI), which varies due to the local instability of steel plates, nonlinearity of the concrete stress-strain curve, and cracking along the height of the column. This chapter presents a methodology for calculating the flexural stiffness of partially encased composite columns by taking these factors into consideration through the incorporation of axial load-moment-curvature relationships. As a first step to the method, the cross-sectional load-moment curve is constructed using the strain compatibility relationship. In the next step, taking the slenderness of column into account, load-moment curve is produced by implementing the Newmark's iterative procedure for computing the second order deflection at mid height of the column. Finally, theory of elasticity is applied to derive the expression for flexural stiffness of the composite column.

3.2 BEHAVIOUR AND ANALYSIS OF SLENDER COLUMNS

A slender column can be defined as a column that has a significantly reduced axial load capacity because of the second order moment resulting from lateral deflections of the column. Figure 3.1 and 3.2 illustrate how the axial load capacity is affected by the lateral deflection.

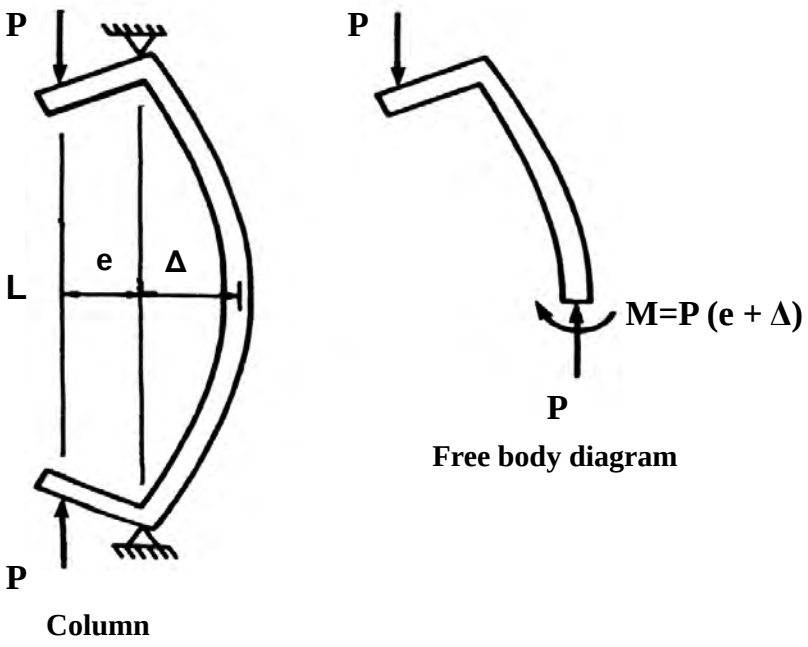

Figure 3.1: Forces in a deflected column

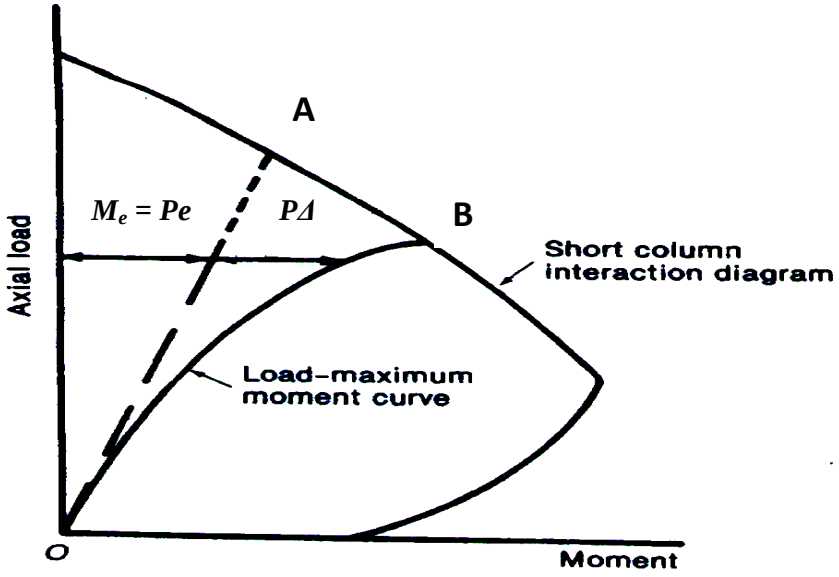

Figure 3.2: Load-Moment interaction diagram of a Column

Figure 3.1 shows a pin-ended column and subjected to eccentric loads. The moments at the ends of the columns are,

$$M=P.e \qquad \ldots(3.1)$$

When the loads P are applied, the column deflects laterally by an amount Δ, as shown in Figure 3.1. For equilibrium, the internal moment at the mid-height must be

$$M = P(e+\Delta) \ \ldots \qquad \ldots(3.2)$$

The deflection increases the moments for which the column must be designed. In the symmetrical column shown here, the maximum moment occurs at mid-height, where the maximum deflection occurs.

Figure 3.2 shows an interaction diagram for a reinforced concrete column. This diagram gives the combinations of axial load and moment required to cause failure of a column cross section or a very short length of column. The dashed radial line OA is a plot of the end moment on the column in Figure 3.1. Because this load is applied at a constant eccentricity, e, the end moment, M_e, is a linear function of P, given by Equation (3.1). The curved solid line OB is the moment M at mid-height of the column, given by Equation (3.2). At any given load P, the moment at mid-height is the sum of the end moment, Pe, and the moment due to second order deflections, $P\Delta$. The line OA is referred to as a load-moment curve for the end moment, while the line OB is the load-moment curve for the maximum column moment.

Failure occurs when the load-moment curve OB for the point of maximum moment intersects the interaction diagram for the cross section. Thus the load and moment at failure are denoted by point B in Figure 3.2. Because of the increase in maximum moment due to second order deflections, the axial-load capacity is reduced from A to B. This reduction in axial load capacity results from what is referred to as slenderness effects.

Lateral deflections of a slender column cause an increase in the column moments, as illustrated in Figures 3.1 and 3.2. These increased moments cause an increase in the deflections, which in turn lead to an increase in the moments. As a result, the load-

moment line OB is Figure 3.2 is nonlinear. If the axial load is below the critical load, the process will converge to a stable position. If the axial load is greater than the critical load, it will not. This is referred to as a second order process, because it is described by a second order differential as,

$$EI\frac{d^2y}{dx^2} = Py \qquad \ldots (3.3)$$

The elevation and cross-section of the PEC column and the additional second order deflection and imposed moment is shown in Figure 3.3.

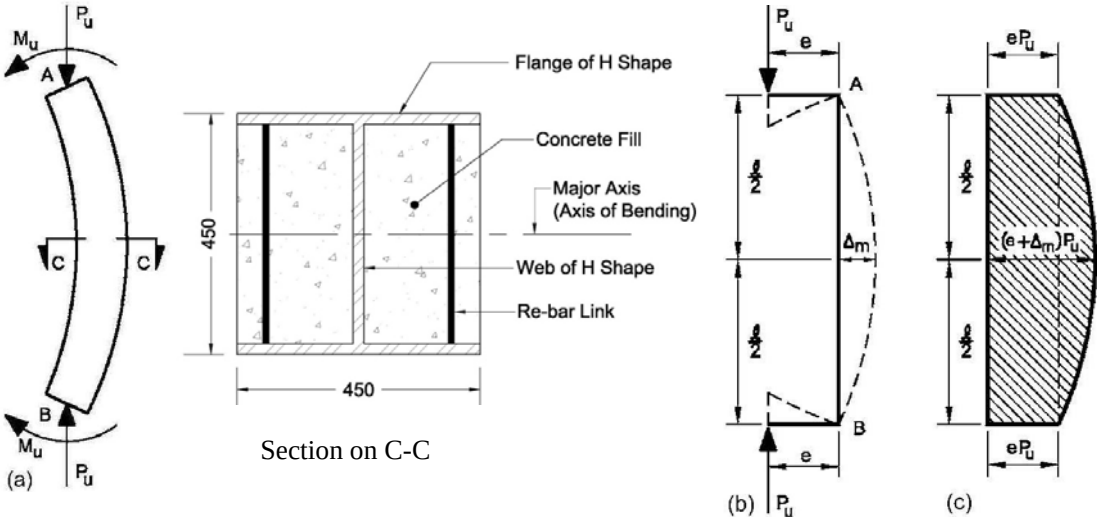

Figure 3.3: Type of Partially Encased Composite Column with
(a) free-body diagram of pin-ended column in symmetrical single -curvature bending;
(b) Forces on column; and
(c) Bending moment diagram ($M_u=eP_u$)

3.3 FORMULATION OF CROSS-SECTIONAL LOAD-MOMENT INTERACTION DIAGRAM

The strength of a composite cross section was represented by an axial load-bending moment interaction diagram, similar to the one shown in Figure 3.2. This curve for

the partially encased composite column section was generated using the similar procedure adopted for reinforced concrete columns. A strain-compatibility and force-equilibrium solution was used. Similar procedure has been adopted by Bouchereau and Toupin (2003) and Prickett and Driver (2006) to predict the capacity of eccentrically loaded PEC columns (as described in sections 2.3.3 & 2.3.4 in Chapter 2). In calculating the design capacity the reduced steel area was used to account for the local buckling of the flanges, since local buckling was observed to be critical for eccentrically loaded columns (Prickett and Driver 2006). A linear strain distribution along the cross-section was implemented for the construction of the cross-section strength curve. The extreme compressive strain was set at 3500 με (considered to be the crushing strain of concrete), whereas the extreme tensile strain was varied from 0 to 10 times the yield strain of the steel. For each strain gradient the ultimate load and moment capacities were calculated from the material and geometric properties of the composite cross-section. To calculate the contribution of the steel to the capacity of the composite column, the section was discretised in such a way as to have effectively uniform strain in each individual piece. For strong axis bending, the flanges were considered to be one piece, whereas the web was divided into ten pieces. The resultant force for each individual piece was calculated by multiplying the area of the piece by its average strain and by the elastic modulus of steel. (However, if the strain in the individual piece exceeded the yield strain the force resultant is determined by multiplying the area of that piece by the yield stress.) Finally, the total load capacity of the composite column was determined by adding the force resultants for concrete and steel and the moment capacity were obtained from the summation of each force multiplied by its distance from the centerline of the column cross-section.

The maximum bending moment for the cross sectional moment curvature curve (M_{cs}) for a given axial load level (P_u) defined one point on the cross section strength interaction diagram. Eleven points (axial load levels) were used to accurately define the entire cross sectional strength interaction diagram. M_{cs} could then be interpolated from the generated cross-section strength curve for a desired end eccentricity ratio (e/d), where e = end eccentricity and d = overall depth of the composite cross section.

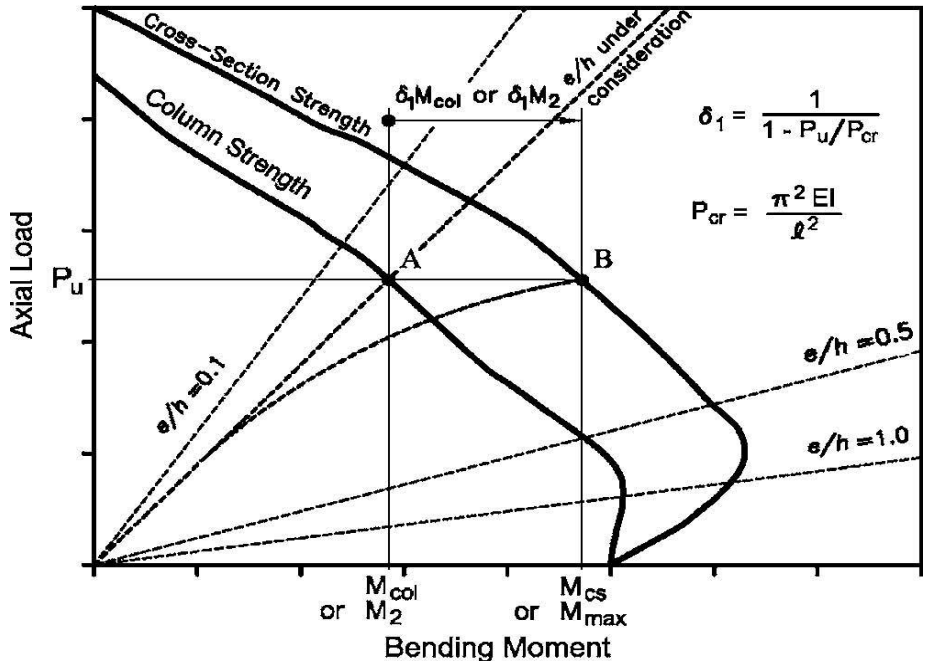

Figure 3.4: Schematic diagrams for cross-sectional strength and column strength curve for a composite column

3.4 FORMULATION OF SLENDER COLUMN LOAD-MOMENT INTERACTION DIAGRAM

The strength of a slender pin-ended composite column subjected to end moments producing symmetrical single curvature bending was also represented by an axial load-bending moment interaction diagram, as shown in Figure 3.4. The column bending moment capacity M_{col}, or the end moment M_2, for a given axial load was calculated using a numerical iterative procedure that computed second-order bending moments and deflections along the length of the column by incrementing the end moments until the maximum moment along the length of the column reached the maximum moment on the cross section moment-curvature curve for the given axial load. The column axial load strength P_u and the corresponding computed value of M_{col} represented one point on the column *P–M* interaction curve (Figure 3.4).

Newmark's method (1943) was used to determine the equilibrium configuration for a given combination of axial load and end moments that were applied to the slender

column. The column was subdivided into segments or stations of equal length for which initial deflections were assumed based on the applied end moments. The first-order moments, and the second-order moments caused by slenderness effects, were computed and summed at each station.

The curvature corresponding to the total moment at each station was retrieved from the cross section moment-curvature curve for the given axial load level in order to define the distribution of curvature along the column length. The conjugate beam method was then used to compute the deflection at each of the stations in an iterative manner. If the computed deflections and the initial deflections were within the prescribed limits of 0.05%, an equilibrium solution had been obtained. If not, the computed deflections were substituted for the assumed deflections and the process was repeated until the deflections converged. The end moments were then incremented equally and the process was repeated until the maximum bending moment (M_{max}) calculated along the length of the member reached the maximum moment on the cross section moment-curvature curve for the axial load under consideration. This procedure was also used by Ali and Begum (2012) for developing column strength curve for slender PEC columns. Ali (2012) validated this process for evaluating the slender PEC column strength with the experimental results by Chicoine *et al*. (2000).

The maximum end moment M_{col} (M_2) corresponding to M_{cs} (M_{max}) for each axial load level was stored to define the entire interaction diagram for the slender column. A total number of nine points (axial load levels) has been used to define the slender column interaction diagram. The computed values of M_{cs} and M_{col} for each column (with l and P_u for given e/d ratios) were then used directly in Equation (3.11) to compute the theoretical EI.

The major assumptions used in determining the axial load-moment-curvature ($P–M–Ø$) relationship, M_{cs} and M_{col} are as follows:

1. Strains between concrete and structural steel are compatible and no slip is allowed;
2. Strain is linearly proportional to the distance from the neutral axis;
3. Concrete and steel stresses are functions of strains;
4. Confinement of concrete provided by lateral ties and the structural steel section is

not considered;

5. Effects of residual stresses and local imperfections in the steel section is not considered since Begum *et al*. (2007) reported that the effect of these two parameters have negligible effect on the capacity and failure of these columns.
6. Strain hardening of steel is neglected.

3.5 EVALUATION OF THEORETICAL FLEXURAL STIFFNESS

ACI 318-02 permits the use of a moment magnifier approach to compute the maximum bending moment (M_{max}), which includes second-order effects, occurring along the height of a column,

$$M_{max} = M_c = \delta_{ns} M_2 = C_m \delta_{ns} M_2 \geq M_2 \quad \ldots (3.4)$$

where δ_{ns} = moment magnifier for columns that are part of braced (non-sway) frames; M_2=larger of the two factored end moments (M_1 and M_2) computed from a conventional elastic frame analysis and is always taken as positive; C_m = equivalent uniform moment diagram factor; and δ_1 =moment magnifier for the same columns when subjected to axial load and equal and opposite (equivalent) end moments causing symmetrical single curvature bending. For this study M_1 and M_2 are equal and opposite causing symmetric single curvature bending; therefore, C_m =1.0.

Chen and Lui (1987) explained that the moment magnifier δ_1 for pin-ended columns subjected to end moments can be derived from the basic differential equation governing the elastic in-plane behavior of a column and is reproduced in the following equation,

$$\delta_1 = \sqrt{\frac{2(1-\cos kl)}{\sin^2 kl}} \quad \ldots (3.5)$$

Where, l = column length; and k = lowest Eigen-value solution to the basic differential equation of equilibrium

$$k = \frac{\pi}{l}\sqrt{\frac{P_u}{P_{cr}}} \quad \ldots (3.6)$$

Where, P_u = factored axial load acting on the column; and P_{cr} = Euler's buckling

strength for a pin-ended column which is given by,

$$P_{cr} = \frac{\pi^2 EI}{l^2} \qquad \ldots (3.7)$$

For design purposes, the ACI 318-02 has adopted the simplified and widely accepted approximation of Equation (3.2),

$$\delta_1 = \frac{1}{1 - P_u / P_c} \qquad \ldots (3.8)$$

where P_c = critical load and is computed as,

$$P_c = \frac{\pi^2 EI}{(kl)^2} \qquad \ldots (3.9)$$

For this study, however, the effective length factor k=1.0 and P_c is reduced to Euler's buckling strength equation (Equation 3.4) for a pin-ended column.

The moment magnifier method defined by Equations (3.4), (3.8), and (3.9) is described graphically in Figure 3.3, which shows the relationship between the cross section axial load-bending moment strength interaction diagram and the column strength interaction diagram for pin-ended columns in symmetrical single curvature bending. Figure 3.3 shows that, for a given axial load P_u, the column end moment M_2 at point A is multiplied by $\delta_1 (= \Delta_m)$ to obtain M_{max} at point B. The current EI expressions used by ACI 318-02 were developed for use with Equations (3.4), (3.8), and (3.9).

Timoshenko and Gere (1961) gave the bending moment relationship for a pin ended slender column subjected to equal and opposite end moments. This formula is known as the "Secant Formula" which is,

$$M_c = M_2 \sec\left(\frac{\pi}{2}\sqrt{\frac{P_u}{P_{cr}}}\right) \qquad \ldots (3.10)$$

Where, M_c = design bending moment that includes second-order effects; M_2 = applied

column end moment calculated from a conventional elastic analysis; P_u = factored axial load acting on the column; and P_{cr} = Euler's buckling strength (Equation 3.7).

For the purpose of analysis, M_c and M_2 are replaced by the cross sectional bending moment strength M_{cs} and the overall column bending moment strength M_{col} respectively. Substituting Euler's buckling strength from Equation (3.7) into Equation (3.10), then rearranging, simplifying, and solving for *EI* gives the following expression for the theoretical flexural stiffness of a pin-ended column subjected to symmetrical single curvature bending,

$$EI_{th} = \frac{P_u l^2}{4\left[\sec^{-1}\left(\frac{M_{cs}}{M_{col}}\right)\right]} \qquad \ldots (3.11)$$

The computations of the terms P_u, M_{cs}, and M_{col} used in this expression were based on the cross section and column axial load-bending moment (*P–M*) interaction diagrams explained in the following section. Similar procedure for computing EI_{th} for fully encased composite columns were implemented by Tikka and Mirza (1999).

3.6 COMPARISON WITH ACI STIFFNESS EQUATION

The ACI Building code permits the use of following equations for calculating the effective flexural stiffness (*EI*) of slender composite columns [ACI 318-02 Equations (10-21) and (10-12)],

$$EI = \frac{0.2E_c I_g}{(1+\beta_d)} + E_s I_{ss} \qquad \ldots (3.12)$$

$$EI = \frac{0.4E_c I_g}{(1+\beta_d)} \qquad \ldots (3.13)$$

Where E_c and E_s are moduli of elasticity of concrete and steel respectively, I_g and I_{ss} are moments of inertia of the gross concrete cross-section and the structural steel section taken about the centroidal axis of the composite column cross-section; and β_d =the sustained load factor taken as the ratio of the maximum factored axial dead load to the

total factored axial load (for the type of column studied) and is always positive. For short-term loads, β_d =0, and Equations (3.12) and (3.13) are simplified to Equations(3.114) and (3.15) respectively which are as follows,

$$EI = 0.2E_cI_g + E_sI_{ss} \quad \ldots (3.14)$$

$$EI = 0.4E_cI_g \quad \ldots (3.15)$$

Note that in Eqs. (3.12)–(3.15), E_s was taken as 200,000 MPa (29,000,000 psi) and E_c was computed from $4{,}700\sqrt{f'_c}$ MPa ($57{,}000\sqrt{f'_c}$ psi)as specified in ACI 318-08 (2008).

Equations (3.14) and (3.15) were compared with the theoretical *EI* values computed from Equations (3.11) for all simulated composite columns in current study.

3.7 EXAMPLE ON EVALUATING EI FOR PEC COLUMNS

Evaluation of flexural stiffness of typical PEC columns about its major axis is described in this section. The geometric and material properties of the example PEC column are listed below :

Cross sectional dimension = 450 mm × 450 mm
Length, L = 9.0m,
Web and flange thickness, t = 7.50mm,
Link spacing, s = 225mm,
Concrete strength, f'_c = 60 MPa
F_y = 350 MPa.

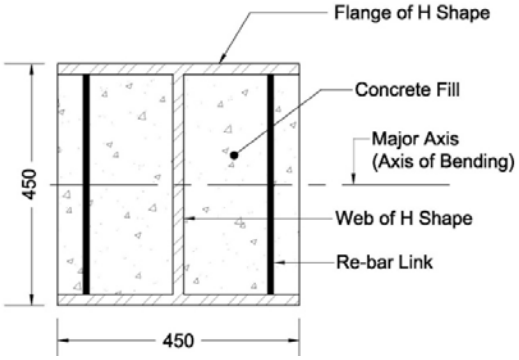

Figure 3.5: Cross section of the example column.

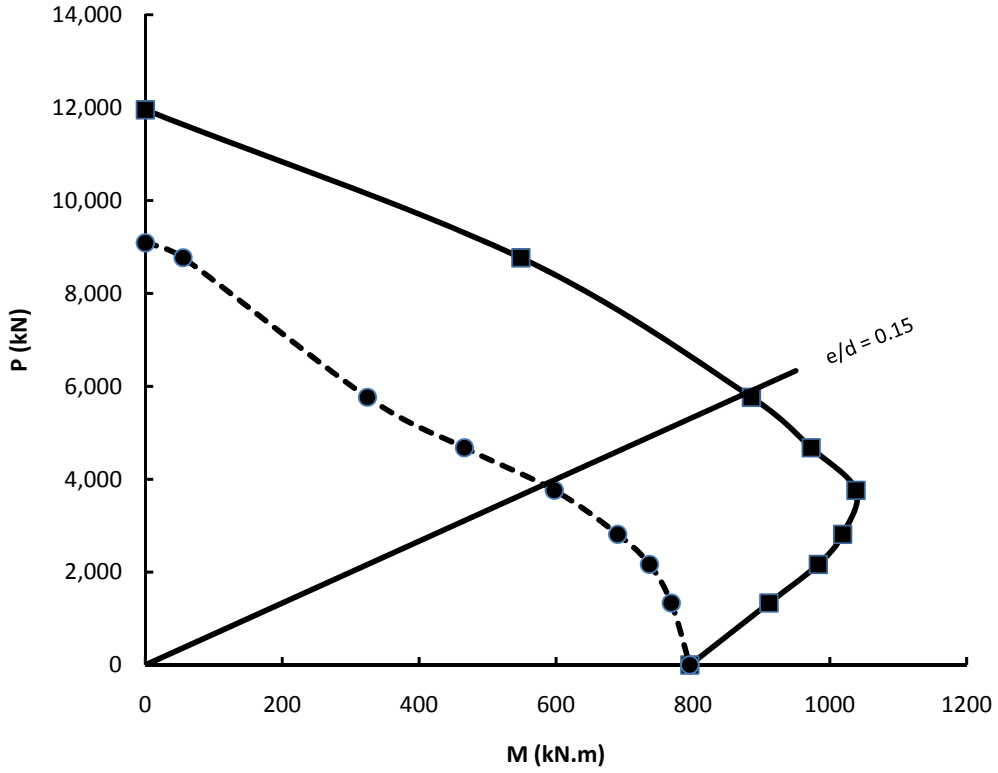

Figure 3.6: Cross sectional strength curve and slender column strength for a randomly chosen example column.

Figure 3.6 shows the two column interaction diagrams derived from the methodology described in the previous sections. One of them is the cross sectional strength curve which is derived from strain-compatibility and force-equilibrium. The other one is slender column strength curve which is derived with the use of Newmark's method.

For this example, an eccentricity to depth ratio e/d = 0.15 is randomly chosen. The corresponding maximum axial strength and flexural strength for the two curves are as follows:

Axial strength from cross sectional strength curve, P_{cs} = 3950 kN
Flexural strength from cross sectional strength curve, M_{cs} = 1040 kN-m
Flexural strength from slender column strength curve, M_{col} = 585 kN-m

Replacing these values in Equation (3.8), we get the theoretical effective flexural stiffness,

$$EI_{th} = \frac{3950 \times 9^2}{4\left[\sec^{-1}\left(\frac{1040}{585}\right)\right]} = 82038 \text{ kN-m}^2$$

The effective flexural stiffness suggested by ACI can be computed from inputting the values in equation 3.11.

$$EI_{ACI} = 0.2 \times 16740 \times 3417187500 + 200000 \times 381900234.375$$
$$= 87821 \text{ kN-m}^2$$

Therefore, the deviation of the studied theoretical effective flexural stiffness from ACI stiffness is,

$$\frac{EI_{ACI}}{EI_{th}} = \frac{87821 - 82038}{82038} \times 100 = 7.05\ \%$$

In the described way a total number of 1200 EI_{th} is generated for parametric study (as presented in chapter 4) and compared with the ACI equation. Also, a regression analysis is performed and a regression equation is formulated for EI_{th} which has been described in chapter 5 of this thesis.

Chapter 4

PARAMETRIC STUDY

4.1 INTRODUCTION

An extensive study has been conducted in order to observe the effects of different parameters on slender partially encased composite columns. A total number of 120 isolated steel-concrete PEC columns are simulated for this study. All the columns are hinged at both ends and are subjected to bending about the major axis of the steel section. Each column has a different combination of specified properties. The parameters which are likely to have the greatest effect on the behaviour of slender PEC columns are selected. The selection of the variable parameters and design of the parametric study, along with a discussion of the results, are presented in subsequent sections.

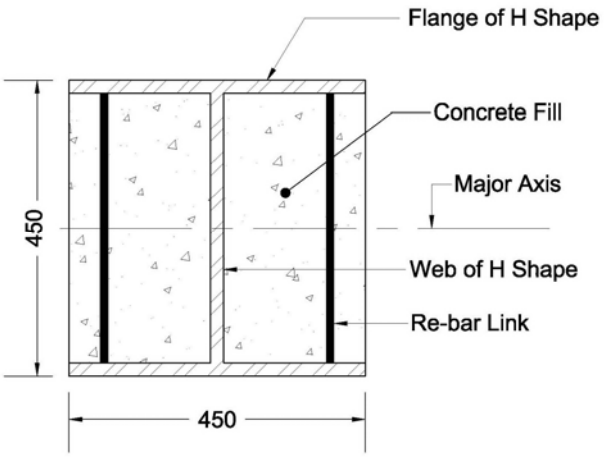

Figure 4.1 Cross-section of PEC column for parametric study

4.2 SELECTED PARAMETERS

The geometric and material properties of slender PEC columns that can significantly affect their stability and stiffness under axial compression and major axis bending are

identified as potential variables in the parametric study. Among these, the column cross-sectional dimensions (b_f or b and d), length of the column (L), longitudinal spacing of the transverse links (s), thickness of the steel flange and web plates (t) and initial load eccentricity (e) are identified as the most important geometric variables. The compressive strength of concrete and grade of the structural steel are included as the two material variables. The geometric properties listed here are non-dimensionalised for comparison in order to reflect anticipated combined influences. The definition of each parameter, along with its selected range for this study, is presented in turn below.

Overall column slenderness ratio (*L/d*) —The overall column slenderness ratio is defined as the ratio of the total length of the column (L) to the depth of column cross section (d) i.e. L/d ratio. Global bucking behaviour of slender columns is mainly influenced by this parameter. Five different slenderness ratios—10, 15, 20, 25 and 30—are employed in the parametric study.

Initial load eccentricity ratio (*e/d*) —Ten load eccentricity ratios varying from 0.05 to 10 are selected in this study. The load eccentricity ratio of 0.05 is intended to represent an "accidental" eccentricity that might occur in a column that is nominally designed as a gravity column. It is to be noted that for concrete buildings, e/d usually ranges from 0.1 to 0.65.

Flange plate slenderness ratio (*b/t*) — The flange plate slenderness ratio is defined as the ratio of the half-width of the flange (b) to its thickness (t). This parameter is varied between 25 and 35, with an intermediate value of 30. The stiffness and strength of a PEC column is significantly affected by this parameter, since it controls the occurrence of local instability in the flange plate of the column.

Link spacing-to-depth ratio (*s/d*) —The effect of the link spacing is studied by varying the ratio of link spacing (s) to the depth of the column cross-section (d). Two values of the s/d ratio—0.5 and 0.7—are used in the parametric study. Link spacing is also an important parameter affecting the stability of these columns, since local buckling in the flange plates occurs between two successive links.

Compressive strength of concrete (f'_c) — In the parametric study, the concrete strength is varied from 30 MPa to 60 MPa to investigate the influence of high strength concrete in combination with other parameters.

Grade of Structural Steel (F_y) — The yield strength of the structural steel shape is varied between 250 MPa and 350 MPa which are the most common grades used in the construction of composite columns.

Table 4.1 summarises the range of variables under each parameter used in this study. In designing the parametric study, the cross sectional size of the columns is selected to be constant and all the parameters are varied accordingly. The parameters are combined in an optimum and systematic way to obtain their individual effects as well as interrelationships. For current study, the overall dimensions of the composite cross section were held constant at 450×450 mm (18 ×18 in.) since previous parametric studies concluded that the overall cross section size was not a major variable for investigating the reliability of strength and stiffness of composite columns (Mirza 1999). The clear concrete cover on lateral ties was held constant at 38 mm (1.5 in.) for this study. The cross-section and elevation of typical parametric columns are shown in Figure 4.2.

The theoretical *EI* for each of the columns studied was computed from Equation 3.8 as shown in Chapter 3 using M_{cs} from the cross section strength interaction diagram and M_{col} from the slender column interaction diagram.

Table 4.1: Specified properties of PEC columns studied

Properties	Specified values	Number of specified values
L/d	10, 15, 20, 25, 30	05
e/d	0.1, 0.2, 0.3, 0.4, 0.5, 0.6, 0.7, 0.8, 0.9, 1	10
b/t	25, 30, 35	03
s/d	0.5, 0.7	02
f'_c , *MPa*	30.0, 60.0	02
F_y , *MPa*	250.0, 350.0	02

4.3 EFFECTS OF DIFFERENT PARAMETERS ON *EI* OF PEC COLUMNS

4.3.1 Effect of Slenderness Ratio *L/d*

Length to depth ratio (*L/d*) plays an important role in the evaluation of flexural stiffness *EI* of a slender partially encased composite column. The overall stability is controlled by the slenderness ratio which is defined as the ratio of the total length of the column (*L*) to the depth of column cross section (*d*) i.e. *L/d* ratio which can also be denoted by overall column slenderness ratio. For parametric study, five values of *L/d* ratio (10, 15, 20, 25 and 30) are used. The effect of *L/d* incorporation with other parameters such as *s/d*, *b/t*, f'_c and f_y on flexural stiffness (*EI*) of a slender PEC column is described in the following sections.

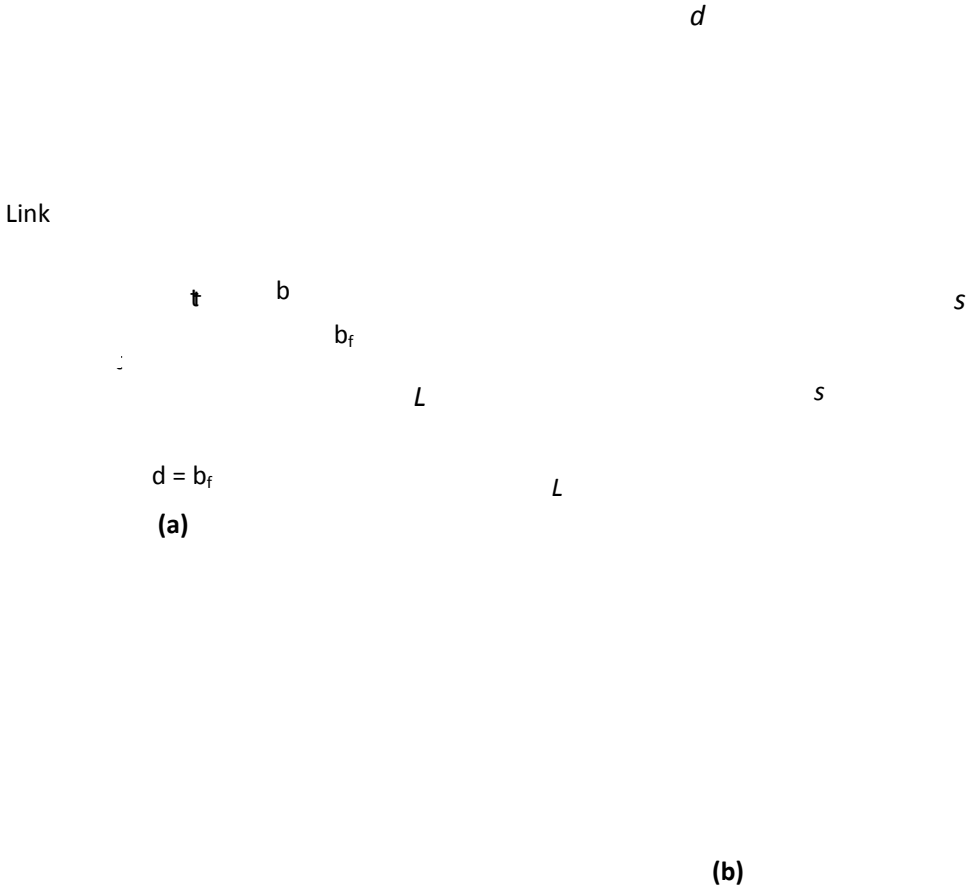

Figure 4.2 Typical parametric column (a) cross-section; and (b) elevation

Effect of L/d with varying b/t ratio

Figure 4.3 shows variation of *EI* with *L/d* ratios for the three different values of plate slenderness ratio (*b/t*) for a low *e/d* ratio of 0.1. Other variables are arbitrarily kept constant at *s/d* = 0.5, f'_c= 60 MPa and F_y =350 MPa. Figure 4.4 shows the same variation for *e/d*= 0.55 and Figure 4.5 shows it for a high *e/d* ratio of 1.0. Tables 4.2, 4.3 and 4.4 show the tabular form of corresponding data.

From the tables and figures, it can be deduced that,

- For all the values of *b/t* (25, 30 & 35), stiffness *EI* increases with an increase in *L/d* ratio. The reason behind the increase in *EI* with increasing *L/d* ratio may be due to the fact that the cracks in a longer column are likely to be more widely spaced with more concrete in between the cracks. This concrete contributes to the effective flexural stiffness *EI* of the PEC column which results in increased *EI* values. This phenomenon resembles the research work performed by Tikka and Mirza (1999) with fully encased slender composite columns. Moreover, at very high *L/d* (such as *L/d*=30), the degree of stability of PEC columns reduces which causes a reduction in the rate of increase in *EI*.
- At a low eccentricity ratio of 0.1, *EI* increases by 28% for varying the *L/d* ratio from 10 to 30 for *b/t*=25, whereas for *b/t* = 30 and 35, *EI* values increase 25% and 26% respectively (Table 4.2). These figures are very close which indicates that the effect of *L/d* ratio on *EI* is independent of *b/t* ratio at low eccentricities. This is due to the fact that at low eccentricities the local buckling does not affect the slender column behaviour of PEC columns.
- Similar behaviour is also observed at a medium *e/d* ratio of 0.55 as shown in Table 4.3. The increase in *EI* for changing the *L/d* ratio from 10 to 30 ranges from 102 to109% for the three selected values of *b/t* ratios. Figure 4.3 and 4.4 also resembles these phenomena. However, Figure 4.4 also shows that the rate of change in EI diminishes at higher *L/d* ratios (i.e. *L/d* ratio over 20).
- On the other hand at very high *e/d* ratio of 1.0, this increment (resulting from changing the b/t ratio from 25 to 35) ranges from 159 to 196%. This range of *EI* is

broader than that observed for low and medium eccentricities. Therefore, it can be inferred that at higher eccentricities (which will induce higher bending moments) the effect of overall column slenderness ratio on *EI* is affected by the flange plate slenderness ratio. The higher bending moments resulting from the high end eccentricities made the column more susceptible to local buckling. Moreover, at higher eccentricities the rate of change in *EI* is higher than that at lower eccentricities (Figure 4.5).

Table 4.2: Effect of L/d ratio with varying b/t values for e/d = 0.1

L/d	10	15	20	25	30	*% difference for L/d=10 to 30*
	EI ($10x^{12}$) Nmm^2					
b/t=25	94	100	107	112	120	*28%*
b/t=30	76	82	86	90	95	*25%*
b/t=35	57	60	63	66	72	*26%*
% difference b/t=25 to 35	*39%*	*40%*	*41%*	*41%*	*40%*	

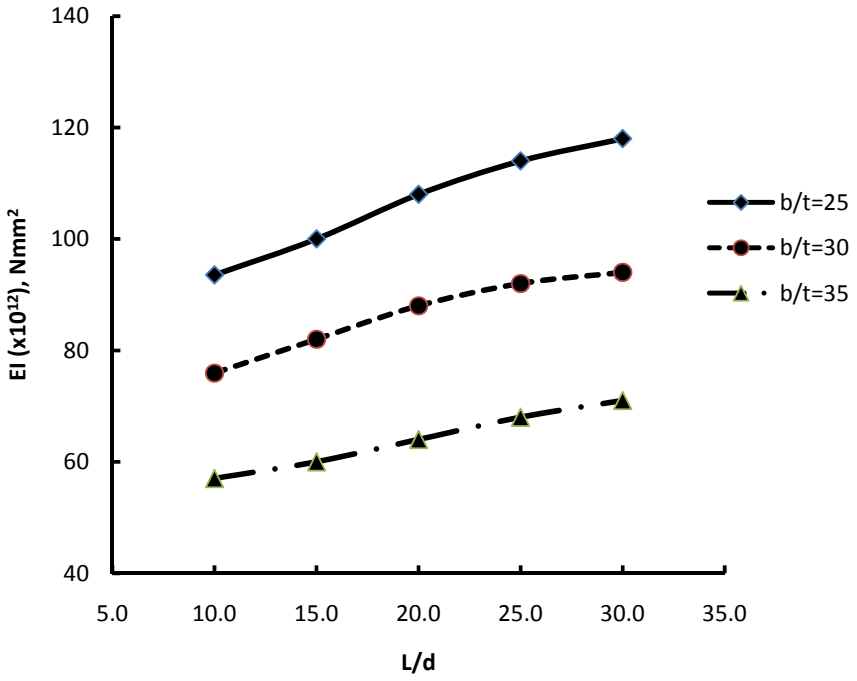

Figure 4.3 EI versus L/d diagram for different values of b/t with e/d =0.1

Table 4.3: Effect of L/d ratio with varying b/t values for e/d = 0.55

L/d	10	15	20	25	30	*% difference for L/d=10 to 30*
	EI ($10x^{12}$) Nmm^2					
b/t=25	53	70	84	96	108	*102%*
b/t=30	46	58	74	85	93	*102%*
b/t=35	34	46	58	67	71	*109%*
% difference b/t=25 to 35	*36%*	*34%*	*31%*	*31%*	*34%*	

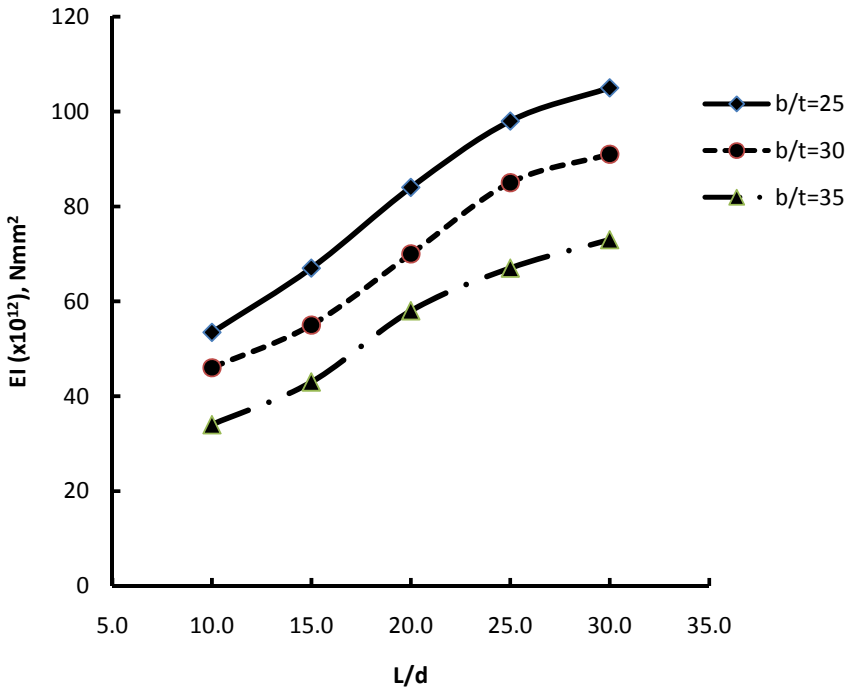

Figure 4.4 EI versus L/d diagram for different values of b/t with e/d =0.55

Table 4.4: Effect of L/d ratio with varying b/t values for e/d = 1.0

L/d	10	15	20	25	30	*% difference for L/d=10 to 30*
	EI ($10x^{12}$) Nmm^2					
b/t=25	34	55	70	*81*	88	*159%*
b/t=30	28	48	*65*	75	81	*189%*
b/t=35	23	40	55	65	68	*196%*
% difference b/t=25 to 35	*32%*	*27%*	*22%*	*20%*	*23%*	

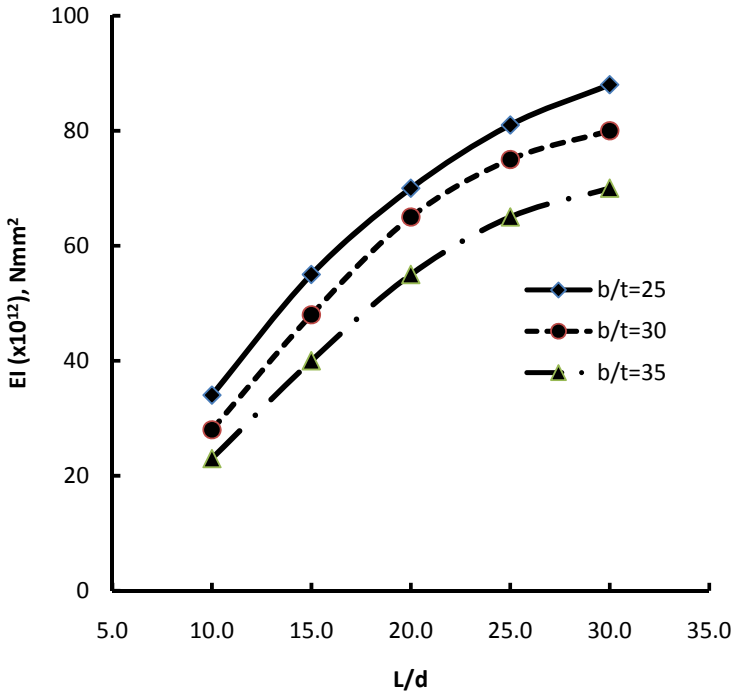

Figure 4.5 EI versus L/d diagram for different values of b/t with e/d =1.0

Effect of L/d ratio with varying s/d

Figure 4.6 shows variation of *EI* with *L/d* ratios for the two different link spacing to depth (*s/d)* ratios for a lower eccentricity ratio *e/d* =0.1. Figure 4.7 shows the same variation for *e/d*= 0.55 and in Figure 4.8 the variation is shown for a high eccentricity ratio *e/d*= 1.0. Other variables are kept fixed at *b/t* = 30, f'_c= 60 MPa and F_y =350MPa. The corresponding data are presented in Tables 4.5, 4.6 and 4.7 respectively.

From the tables and figures, it can be observed that,

- For each value of *s/d* (0.5 and 0.7), flexural stiffness *EI* increases with an increase in *L/d* ratio. Table 4.5 shows that at a low eccentricity ratio of 0.1, *EI* increases by 26% in an average for any value of *s/d* with varying the *L/d* ratio from 10 to 30. At a medium *e/d* ratio of 0.55, this average increase in *EI* is about 110% (Table 4.6) and at a very high *e/d* ratio of 1.0, it is almost 186% (Table 4.7). Therefore, like the previous section, here also it is noticed that at higher eccentricities the rate of change in *EI* with the increase in the *L/d* ratio is higher than that at lower eccentricities. It is also noted that for each value of *e/d* ratio the effects of *L/d* ratio on *EI* is not significantly affected by the *s/d* ratios selected in the current study.
- Comparing these three graphs and their corresponding data, it is also observed that flexural stiffness *EI* decreases with increasing eccentricity which is similar to the behaviour as observed in the preceding section.

Table 4.5: Effect of L/d ratio with varying s/d values for e/d = 0.1

L/d	10	15	20	25	30	*% difference for L/d=10 to 30*
	EI ($10x^{12}$) Nmm^2					
s/d= 0.5	76	82	86	90	95	*25%*
s/d= 0.7	73	80	84	87	93	*27%*
% difference	*4%*	*3%*	*2%*	*3%*	*2%*	

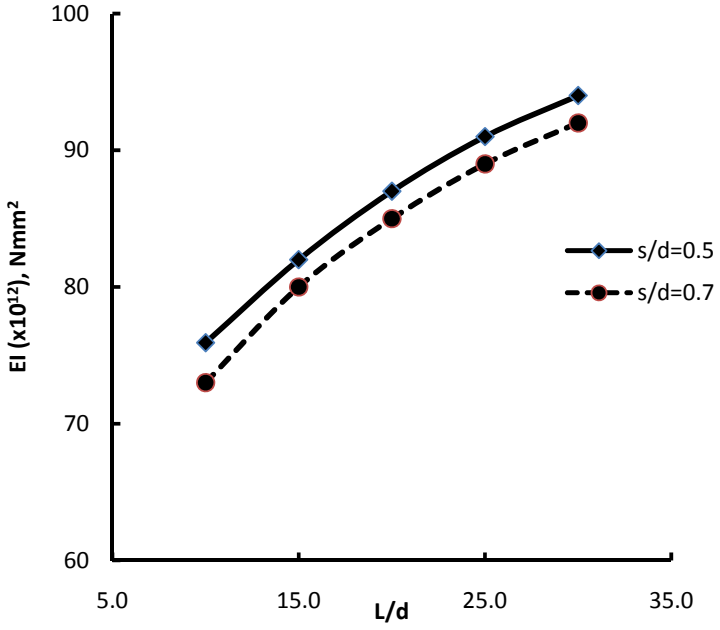

Figure 4.6 EI versus L/d diagram for different values of s/d with e/d =0.1

Table 4.6: Effect of L/d ratio with varying s/d values for e/d = 0.55

L/d	10	15	20	25	30	*% difference for L/d=10 to 30*
	EI ($10x^{12}$) Nmm^2					
s/d= 0.5	43	55	68	76	88	*107%*
s/d= 0.7	40	52	65	72	85	*113%*
% difference	*6%*	*6%*	*5%*	*5%*	*4%*	

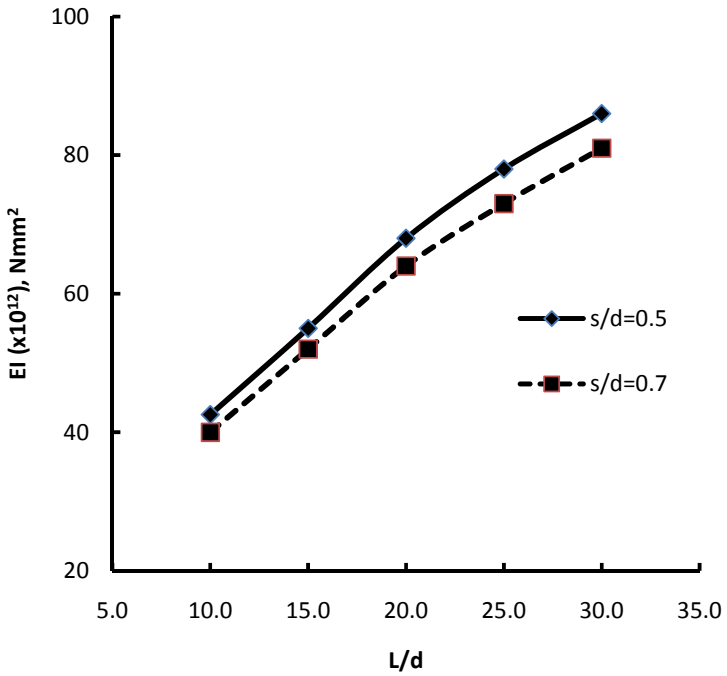

Figure 4.7 EI versus L/d diagram for different values of s/d with e/d =0.55

Table 4.7: Effect of L/d ratio with varying s/d values for e/d = 1.0

L/d	10	15	20	25	30	*% difference for L/d=10 to 30*
	EI ($10x^{12}$) Nmm^2					
s/d= 0.5	28	44	60	70	80	*185%*
s/d= 0.7	26	42	57	66	75	*188%*
% difference	*8%*	*5%*	*5%*	*7%*	*7%*	

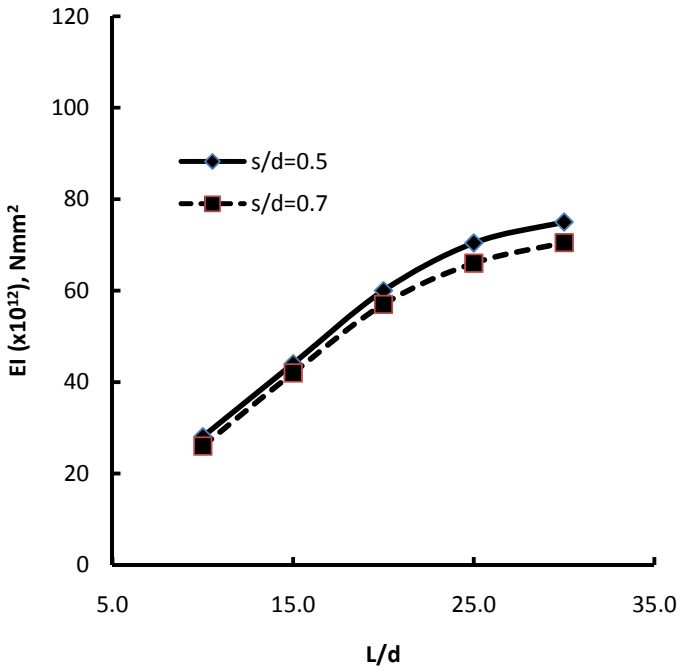

Figure 4.8 EI versus L/d diagram for different values of s/d with e/d =1.0

Effect of L/d with varying f'_c

Figure 4.9 shows variation of *EI* with *L/d* ratios for the two different values of concrete strength f'_c (30MPa and 60MPa) for a lower eccentricity ratio *e/d* =0.1. Figure 4.10 shows the same variation for *e/d*= 0.4 and in Figure 4.11 the variation is shown for a high eccentricity ratio *e/d*= 1.0. Tabular forms of data are also given in Tables 4.8, 4.9 and 4.10. Other variables are kept fixed at *b/t* = 30, *s/d* = 0.5 MPa and F_y =350MPa.

From the tables and figures, it can be observed that-

- For each value of f'_c (30 MPa and 60 MPa), stiffness *EI* rises with an increase in *L/d* ratio. Table 4.8 shows that at low *e/d* ratio of 0.1, average *EI* increase for both the values of f'_c is 21% for increasing *L/d* from 10 to 30. At a medium *e/d* ratio of 0.4, this average increase in *EI* is about 41% (Table 4.9) and at a very high *e/d* ratio of 1.0, it is almost 170% (Table 4.10). Therefore, as discussed in the previous sections, in this case also, it is noticed that at higher eccentricities the rate of change in *EI* is higher than that at lower eccentricities.
- Table 4.8 shows that at low eccentricity (*e/d* = 0.1), the average difference between *EI* for f'_c =30 MPa and *EI* for f'_c =60 MPa is 6%. But from Table 4.10 which represents a high eccentricity (*e/d* = 1.0), this difference is only 2%. From the graphical representation it is also found that for high eccentricity, the two curves for f'_c =30 MPa and 60 MPa are much closer. Therefore, it can be deduced that the effect of f'_c on *EI* at large eccentricity is very negligible. It is because of the fact that in high eccentricities i.e. high flexure, role of concrete in a PEC section becomes less significant.

Table 4.8: Effect of L/d ratio with varying f'_c values for e/d = 0.1

L/d	10	15	20	25	30	*% difference for L/d=10 to 30*
	EI ($10x^{12}$) Nmm^2					
f'_c = 30MPa	72	76	81	85	87	*21%*
f'_c = 60MPa	76	82	86	90	93	*22%*
% difference	*5%*	*7%*	*6%*	*6%*	*6%*	

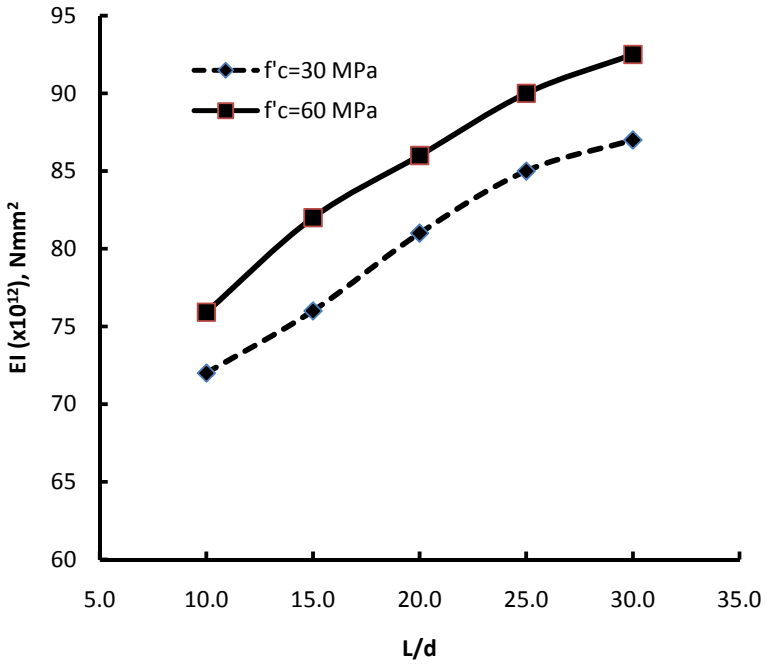

Figure 4.9 EI versus L/d diagram for different values of f'_c with e/d =0.1

Table 4.9: Effect of L/d ratio with varying f'$_c$ values for e/d = 0.4

L/d	10	15	20	25	30	*% difference for L/d=10 to 30*
	EI (10x^{12}) Nmm^2					
f'$_c$ = 30MPa	57	64	71	77	81	*41%*
f'$_c$ = 60MPa	59	65	72	78	82	*40%*
% difference	*3%*	*2%*	*1%*	*1%*	*2%*	

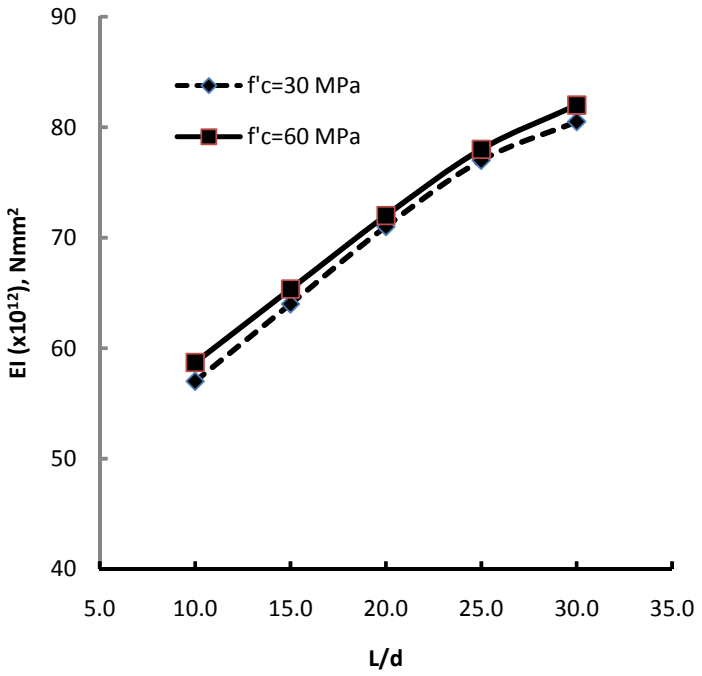

Figure 4.10 EI versus L/d diagram for different values of f'$_c$ with e/d =0.4

Table 4.10: Effect of L/d ratio with varying f'_c values for e/d = 1.0

L/d	10	15	20	25	30	*% difference for L/d=10 to 30*
	EI ($10x^{12}$) Nmm^2					
f'_c = 30MPa	28	43	58	69	73	*165%*
f'_c = 60MPa	28	44	60	70	75	*167%*
% difference	*2%*	*2%*	*3%*	*2%*	*3%*	

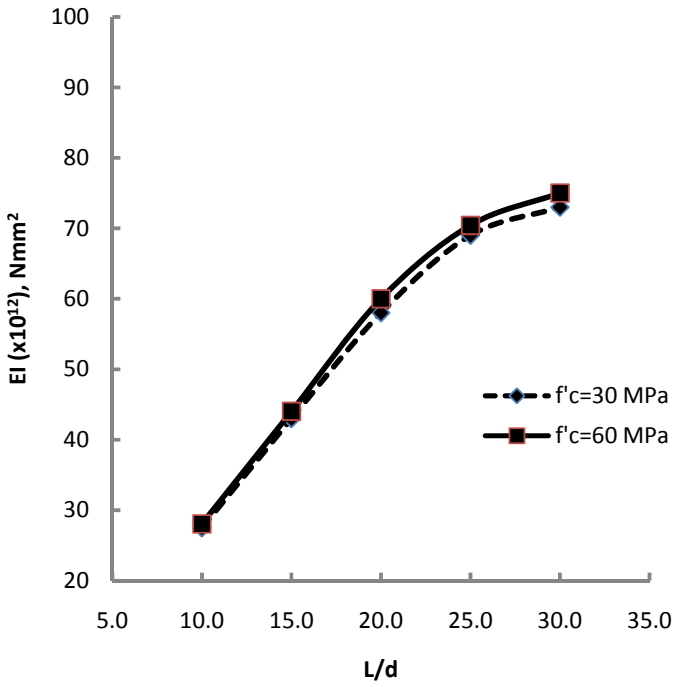

Figure 4.11 EI versus L/d diagram for different values of f'_c with e/d =1.0

Effect of L/d with varying F_y

Figure 4.12 shows variation of *EI* with *L/d* ratios for the two different values of steel yield strength F_y (250MPa and 350MPa) for a lower eccentricity ratio *e/d* =0.1. Figure 4.13 shows the same variation for *e/d*= 0.4 and in Figure 4.14 the variation is shown for a high eccentricity ratio *e/d*= 1.0. Tabular forms of are also given in tables 4.8, 4.9 and 4.10. Other variables are kept fixed at *b/t* = 30, *s/d* = 0.5 MPa and f'_c =60 MPa.

From the tables and figures, it can be observed that-

- For each value of F_y (250 MPa and 350 MPa), stiffness *EI* increases with an increase in *L/d* ratio. Table 4.11 shows that at low *e/d* ratio of 0.1, average *EI* increase for both the values of f'_c is 40% for increasing *L/d* from 10 to 30. At a medium *e/d* ratio of 0.55, this average increase in *EI* is about 108% (Table 4.12) and at a very high *e/d* ratio of 1.0, it is almost 170% (Table 4.13). Therefore, it is noticed that at higher eccentricities the rate of change in *EI* is higher than that at lower eccentricities which is the same phenomenon as observed in the preceding sections.
- All the figures (Figure 4.12, 4.13 and 4.14) show that the two curves for F_y=250 MPa and 350 MPa are very close. That means, the *EI* values are almost same for both the values of F_y. This phenomenon can also be seen from Table 4.11, 4.12 and 4.13 from where it is observed that for all *L/d* ratios, the average increase in *EI* due to varying F_y from 250 MPa is only 2 to 3%. Therefore, it can be inferred that irrespective of any *L/d*, the effect of F_y on *EI* is very negligible.

Table 4.11: Effect of L/d ratio with varying F_y values for e/d = 0.1

L/d	10	15	20	25	30	*% difference for L/d = 10 to 30*
	EI ($10x^{12}$) Nmm^2					
F_y = 250MPa	74	80	84	88	91	*22%*
F_y = 350MPa	76	82	86	90	93	*22%*
% difference	*3%*	*2%*	*2%*	*2%*	*2%*	

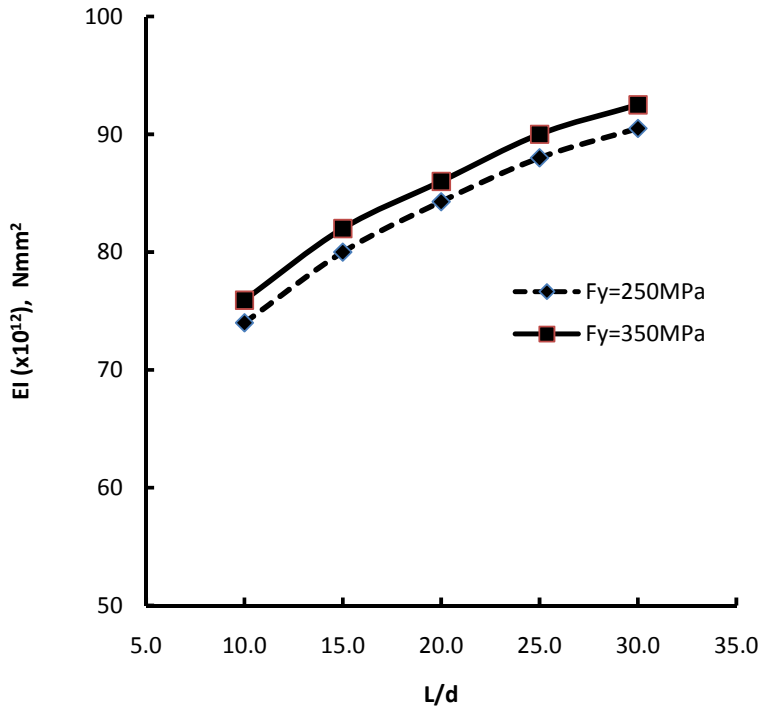

Figure 4.12 EI versus L/d diagram for different values of F_y at e/d =0.1

Table 4.12: Effect of L/d ratio with varying F_y values for e/d = 0.55

L/d	10	15	20	25	30	*% difference for L/d = 10 to 30*
	EI ($10x^{12}$) Nmm^2					
F_y = 250MPa	41	54	66	74	78	*90%*
F_y = 350MPa	43	55	68	76	80	*88%*
% difference	*4%*	*3%*	*3%*	*2%*	*3%*	

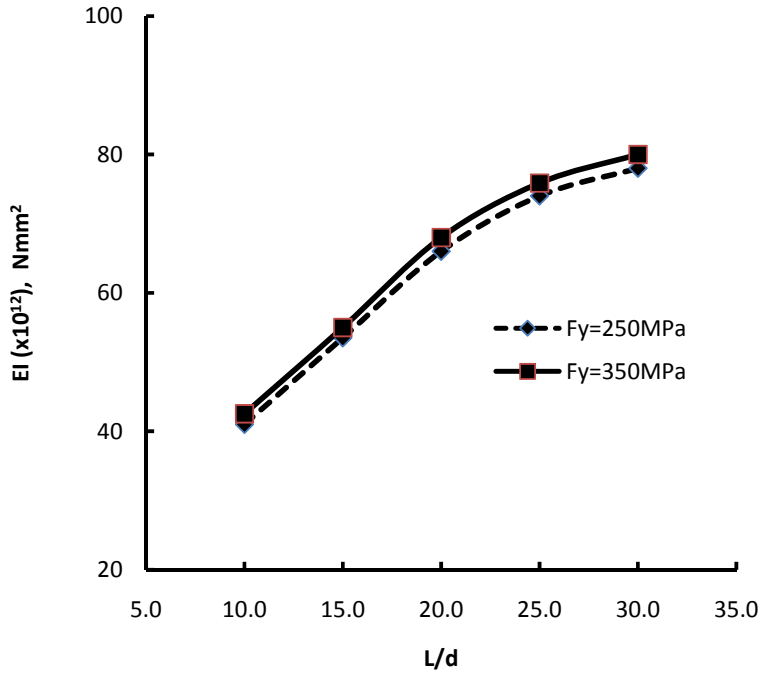

Figure 4.13 EI versus L/d diagram for different values of F_y at e/d =0.55

Table 4.13: Effect of L/d ratio with varying F_y values for e/d = 1.0

L/d	10	15	20	25	30	*% difference for L/d = 10 to 30*
	EI ($10x^{12}$) Nmm^2					
F_y = 250MPa	28	43	59	69	74	*164%*
F_y = 350MPa	27	44	60	70	75	*167%*
% difference	*2%*	*2%*	*2%*	*2%*	*1%*	

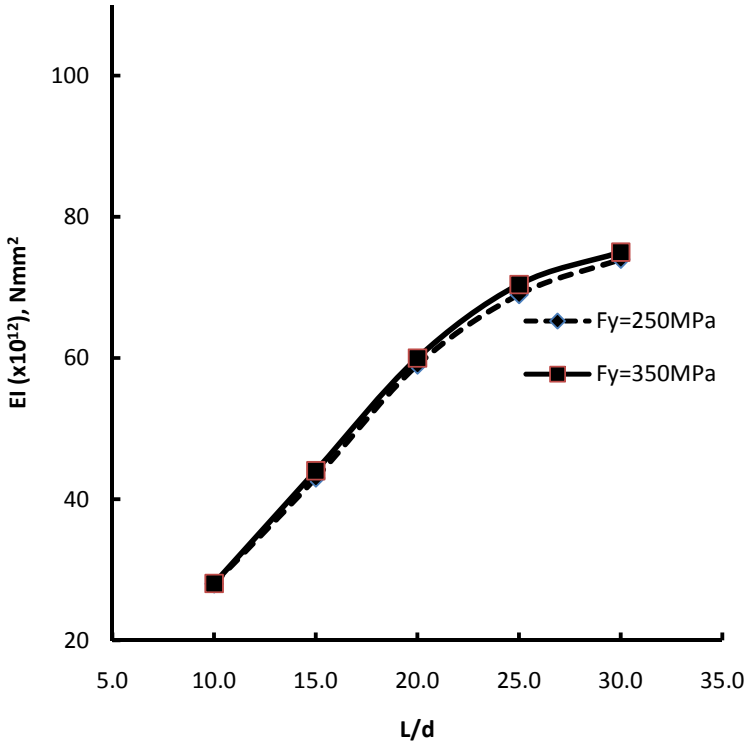

Figure 4.14 EI versus L/d diagram for different values of F_y at e/d =1.0

4.3.2 Effect of Eccentricity to Depth Ratio *e/d*

Load eccentricity at the ends of the column is one of the most important parameters that can affect the theoretical stiffness (*EI)* of PEC columns. In order to get the reflection of the eccentricity effect, the dimensionless geometric operational parameter *e/d* (eccentricity to depth ratio) has been introduced. Effect of load eccentricity ratio on *EI* is studied with respect to the selected range of other variables (i.e. *L/d*, *b/t*, *s/d*, f'_c and F_y).

Figure 4.15 shows variation of *EI* with *e/d* ratios for different values of *L/d*. Figures 4.16, to 4.19 show the same variation for different values of *b/t*, *s/d*, f'_c and F_y respectively. From these figures, it can easily be perceived that the theoretical stiffness does not remain constant with the variation of eccentricity. For all the cases, *EI* decreases significantly with increasing *e/d* values. In other words, with all other parameters being constant, *EI* is high at low eccentricity values and becomes lower at higher eccentricities. This is because, higher eccentricity results in higher end moments which in turn produces higher second order deflection resulting in a reduction in the flexural stiffness of the column.

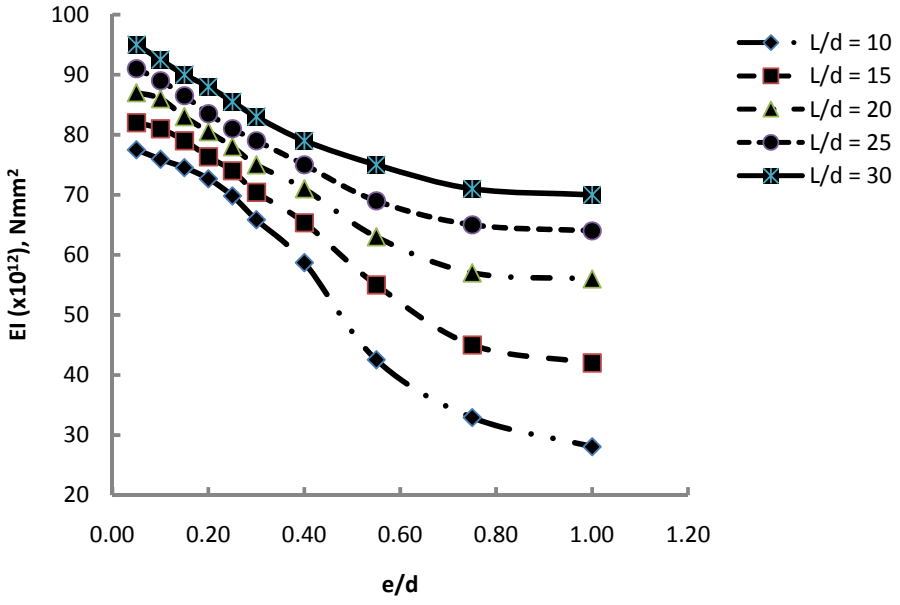

Figure 4.15 EI versus e/d diagram for different values of L/d.
(s/d =0.5, b/t =30, f'_c=60 MPa, F_y= 350 MPa)

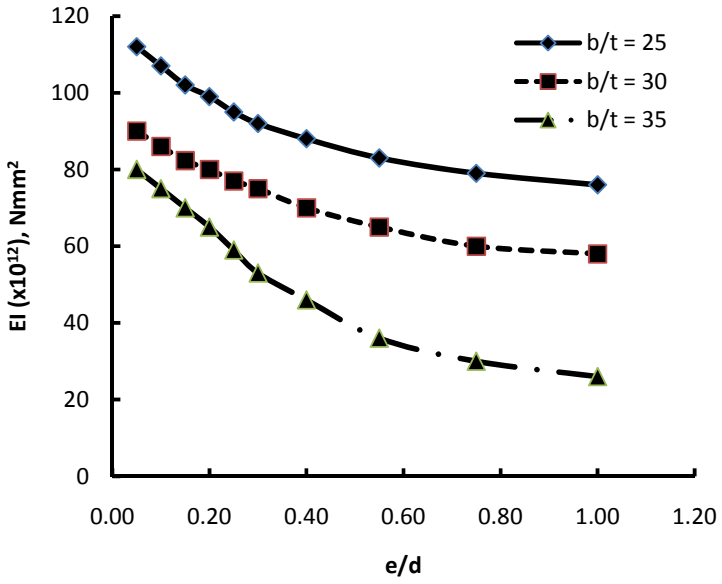

Figure 4.16 EI versus e/d diagram for different values of b/t.
(L/d =20, s/d =0.5, f'_c=60 MPa, F_y= 350 MPa)

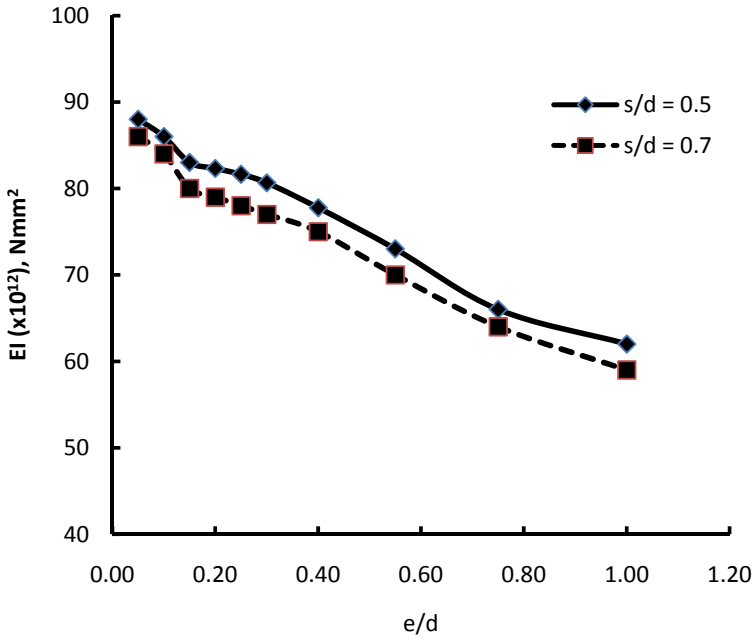

Figure 4.17 EI versus e/d diagram for different values of s/d
(L/d =20, b/t =25, f'_c=60 MPa, F_y= 350 MPa)

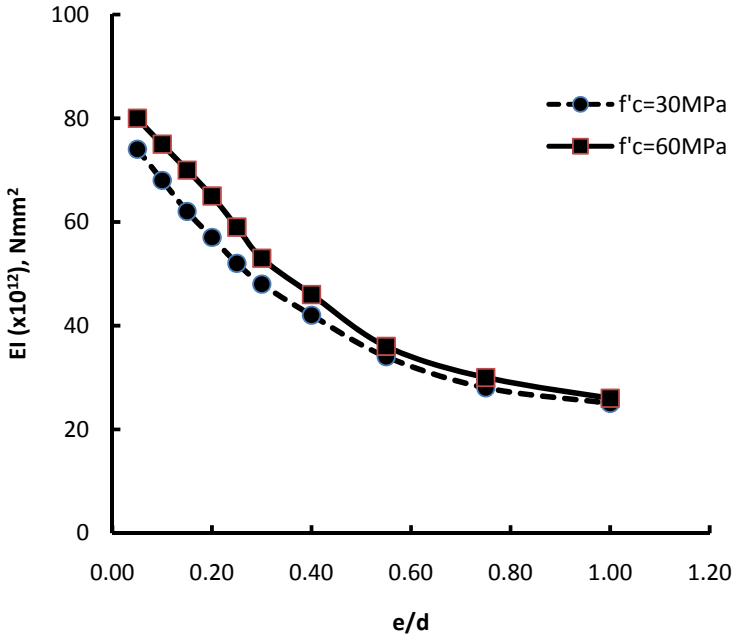

Figure 4.18 EI versus e/d diagram for different values of f'$_c$
(L/d =20, b/t =35, s/d =0.5, F_y= 350 MPa)

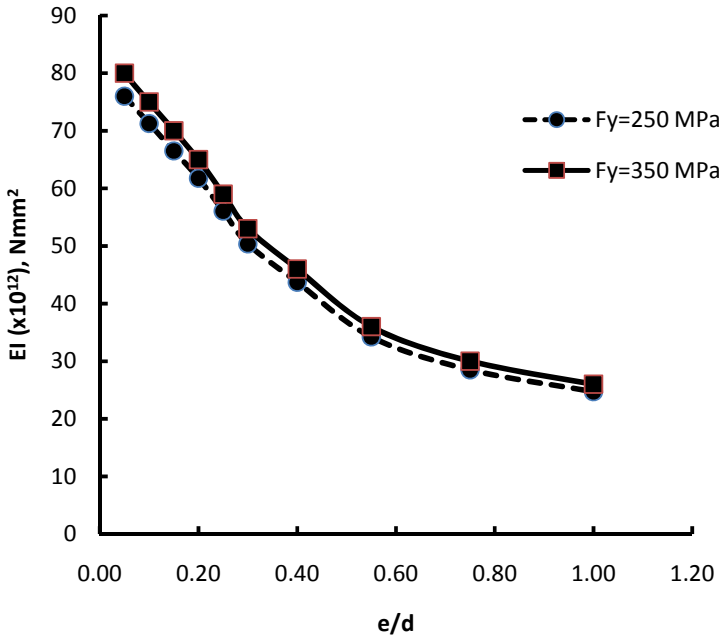

Figure 4.19 EI versus e/d diagram for different values of F_y.
(L/d =20, b/t =35, s/d =0.5, f'$_c$=60 MPa)

Figures 4.15 to 4.19 also show that for lower values of *e/d*, the rate of decrement of *EI* is higher and at higher values of *e/d* the curve appears to become asymptotic. However, for column with *L/d* ratio of 10 and 15 (as shown in Figure 4.15) the rate of decrease in *EI* is lower when *e/d* ratio is less than 0.4 and this rate increases at *e/d* ratio greater than 0.4. It is also observed that flexural stiffness *EI* decreases by 62% for *L/d* = 10, by 25% for *L/d*= 20 and by 17% for *L/d*=30 due to changing *e/d* from 0.1 to 1.0.

Figure 4.16 shows the *EI* versus *e/d* curves for three selected b/t ratios. From this figure it is obvious that at higher *b/t* ratio (=35) the decreasing rate in *EI* is higher as compared to the rate for *b/t* of 25 and 30. The effects of s/d ratio, concrete strength and grade of steel plates are shown in Figures 4.17, 4.18 and 4.19. These factors seemed to have negligible effect on the *EI* versus *e/d* curve for slender PEC columns.

4.3.2 Effect of Flange Plate Slenderness Ratio *b/t*

Compactness ratio i.e. half-flange width to thickness (*b/t*) ratio, in other words, plate slenderness ratio is a significant parameter that affects the flexural stiffness *EI* of a partially encased composite column. The phenomenon of local plate bending is governed by *b/t* ratio. In order to achieve economy in design, non-compact steel sections are commonly used in PEC columns. Degree of compactness of a steel section is controlled by plate slenderness (*b/t*) ratio and therefore plate slenderness ratio plays an important role in stability and overall stiffness of a partially encased composite column member. For parametric study, three values of *b/t* ratio are used in this study, which are 25, 30 and 35.

Figure 4.20 shows a variation of *EI* with *b/t* for the five different values of *L/d* at a low eccentricity (*e/d* =0.1). Figure 4.21, 4.22 and 4.23 show the same variation for different values of *s/d, f'_c and F_y* respectively.

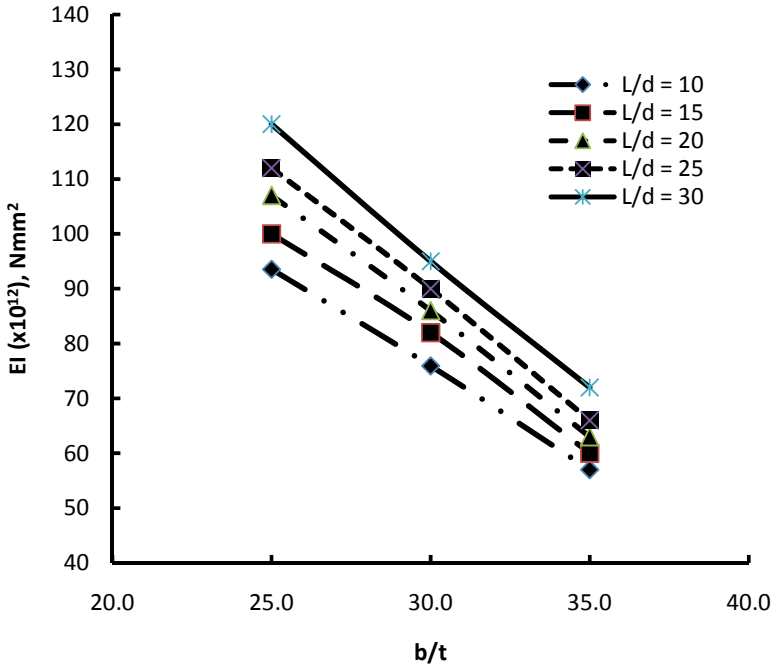

Figure 4.20 EI versus b/t diagram for different values of L/d at e/d=0.1 (s/d =0.5, f'_c=60 MPa, F_y=350 MPa.)

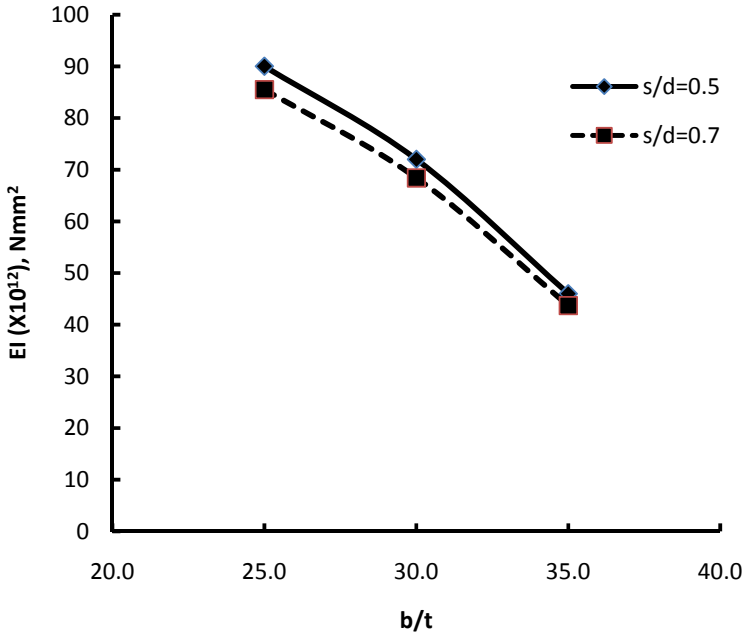

Figure 4.21 EI versus b/t diagram for different values of s/d at e/d=0.4 (L/d =20, f'_c=60 MPa, F_y=350 MPa.)

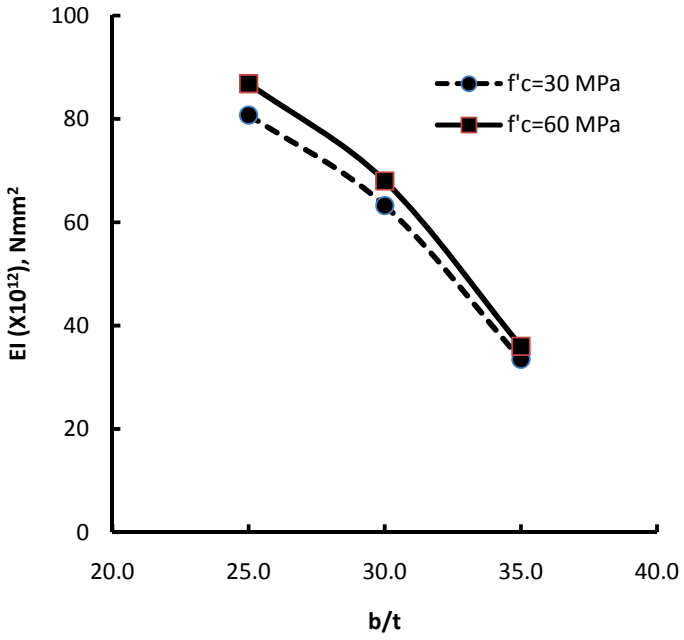

Figure 4.22 EI versus b/t diagram for different values of f'_c at e/d=0.55 (L/d =20, s/d=0.5, F_y=350 MPa.)

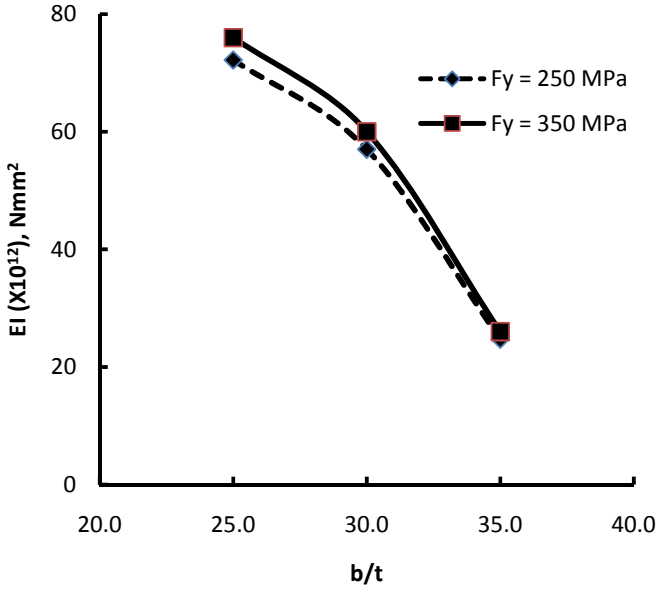

Figure 4.23 EI versus b/t diagram for different values of F_y at e/d=1.0 (L/d =20, s/d=0.5, f'_c=60 MPa.)

Studying the Figures 4.20, 4.21, 4.22 and 4.23, it can be generally concluded that for all combinations with any other parameters, effective flexural stiffness *EI* of the PEC column declines with an increase in *b/t* ratio. This is because of the fact that as *b/t* ratio increases, thickness of flange decreases and thus the probability of local plate bending and warping gets higher. Therefore the overall stiffness of PEC column section decreases with an increase in *b/t* ratio.

The data of Tables 4.2, 4.3 and 4.4 also show that, for a column with slenderness ratio of *L/d*=10, changing the plate slenderness ratio *b/t* from 25 to 35 reduces the *EI* by about 36% for all values *e/d*. Similarly for column with slenderness ratio of 20 and 30, average decrease in *EI* is found to be 31% and 32% respectively. The local buckling in the flange plates of the steel section is the primary reason for the reduction in *EI* with the increase in the *b/t* ratio.

4.3.3 Effect of Link spacing to Depth Ratio *s/d*

In partially encased composite (PEC) columns plain or deformed MS bars are used as horizontal links between flanges of the steel section. These links play an important role in increasing the confinement of the concrete poured between the flange plates. They also prevent local buckling and bending of the flange plates. In order to observe the effect of link spacing (*s*) in a generalised manner, the dimensionless parameter *s/d* (link spacing to depth ratio) has been introduced.

Figure 4.24 shows a variation of *EI* with *s/d* ratio for the different values of *L/d* at *e/d* = 0.1. Figure 4.25, 4.26 and 4.27 show the same variation for different values of *b/t, f'$_c$ and F$_y$* respectively at other different *e/d* ratios.

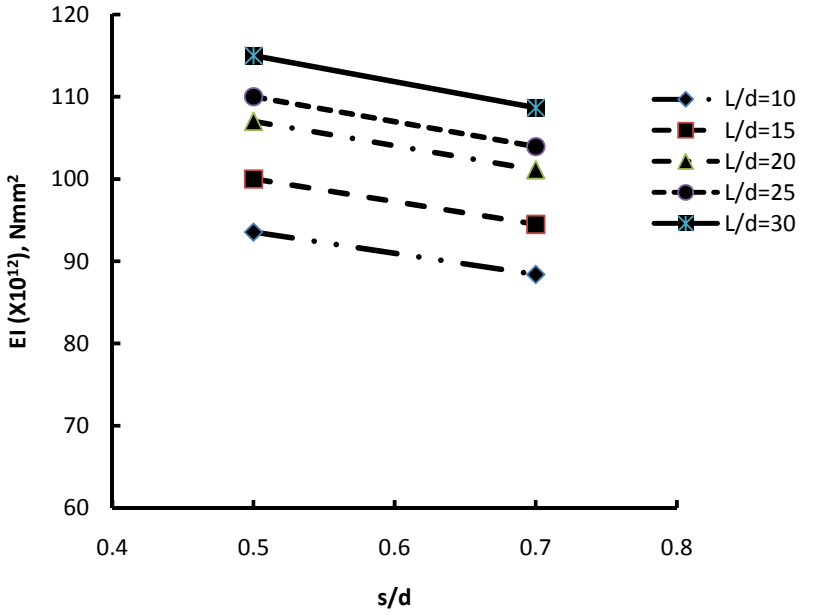

Figure 4.24 EI versus s/d diagram for different values of L/d at e/d=0.1 (b/t =25, f'_c=60 MPa and F_y=350 MPa.)

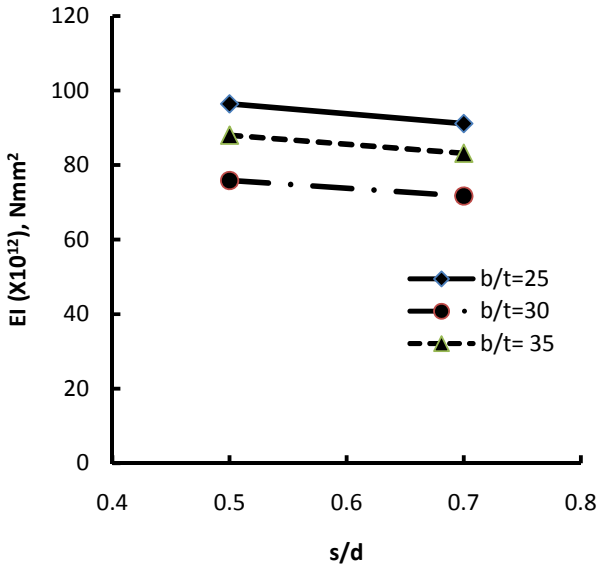

Figure 4.25 EI versus s/d diagram for different values of b/t at e/d=0.55 (L/d =25, f'_c=60 MPa and F_y=350 MPa.)

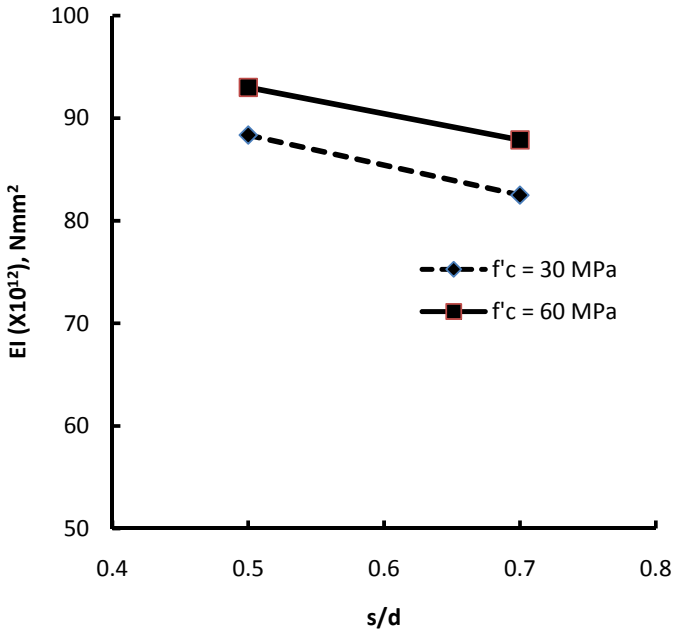

Figure 4.26 EI versus s/d diagram for different values of f'$_c$ at e/d=0.3 (L/d =20, b/t=30 and Fy=350 MPa)

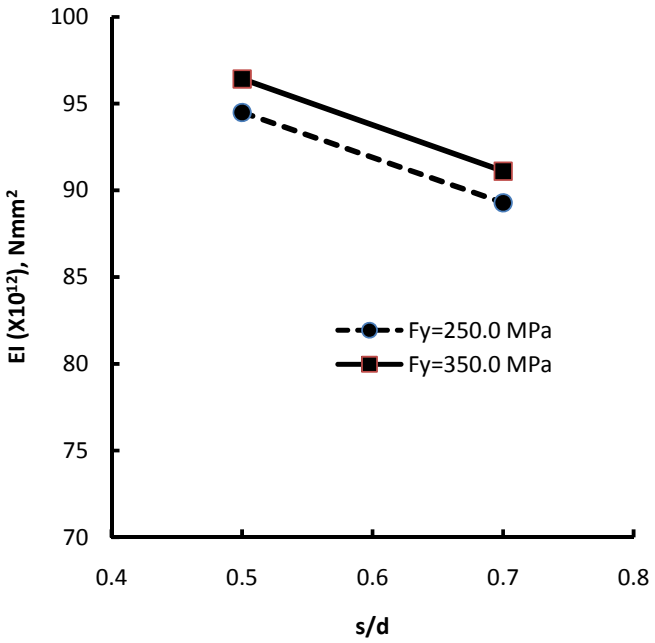

Figure 4.27 EI versus s/d diagram for different values of F_y at e/d=0.55 (L/d =25, b/t=25 and f'$_c$=60 MPa)

Studying the observations on *s/d* ratio, it can generally be concluded that for all combinations with any other parameters, effective flexural stiffness *EI* of the PEC column declines by a little amount with increasing *s/d* ratio from 0.5 to 0.7. The reason is as *s/d* increases, vertical spacing between transverse re-bar links goes higher and thus confinement of concrete between flanges decreases. Moreover an increase in link spacing also increases the probability of local flange plate bending and warping. Therefore the overall stiffness of PEC column section decreases with an increase in *s/d* ratio. However, this decrease in stiffness is very little and can be neglected.

Moreover, from the data provided in Tables 4.5, 4.6 and 4.7, it is found that for a column with slenderness ratio of *L/d*=10, changing the *s/d* ratio from 0.5 to 0.7 reduces the *EI* by about 6% for all values *e/d*. Similarly for column with slenderness ratio of 20 and 30, average decrease in *EI* is found to be 3% and 4% respectively.

4.3.4 Effect of Compressive Strength of Concrete f'_c

Compressive strength of concrete f'_c plays an important role in the load carrying capacity of concrete. Therefore it affects the required column size and subsequently the amount of steel required for a particular combination of axial and flexural load. In the parametric study the concrete strength was varied from 30 MPa to 60 MPa in order to investigate the influence of concrete strength in combination with other parameters.

Figure 4.28 shows variation of *EI* with f'_c values for the different values of *L/d* at *e/d* = 0.25. Figure 4.29, 4.30 and 4.31 show the same variation for different values of *b/t, s/d and* F_y respectively at random *e/d* ratios.

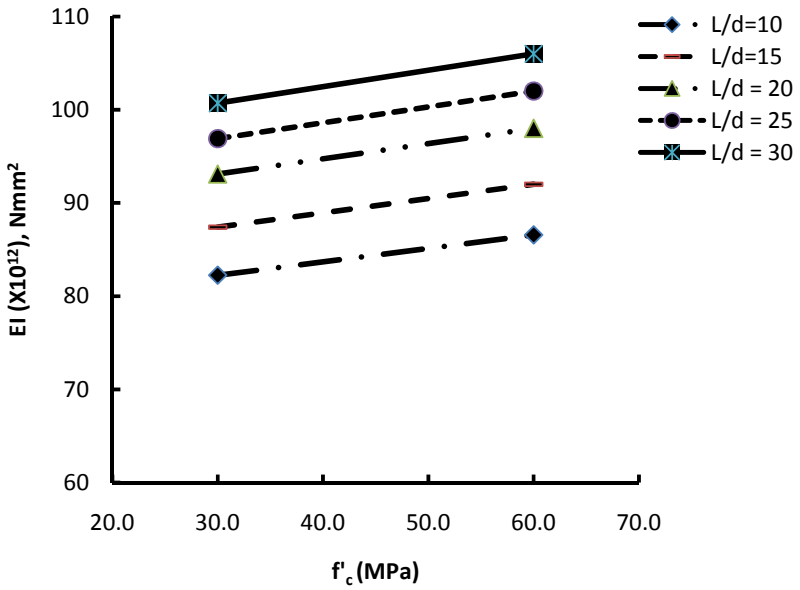

Figure 4.28 EI versus f'_c diagram for different values of L/d at e/d=0.25 (b/t =25, f'_c=60 MPa and F_y=350 MPa.)

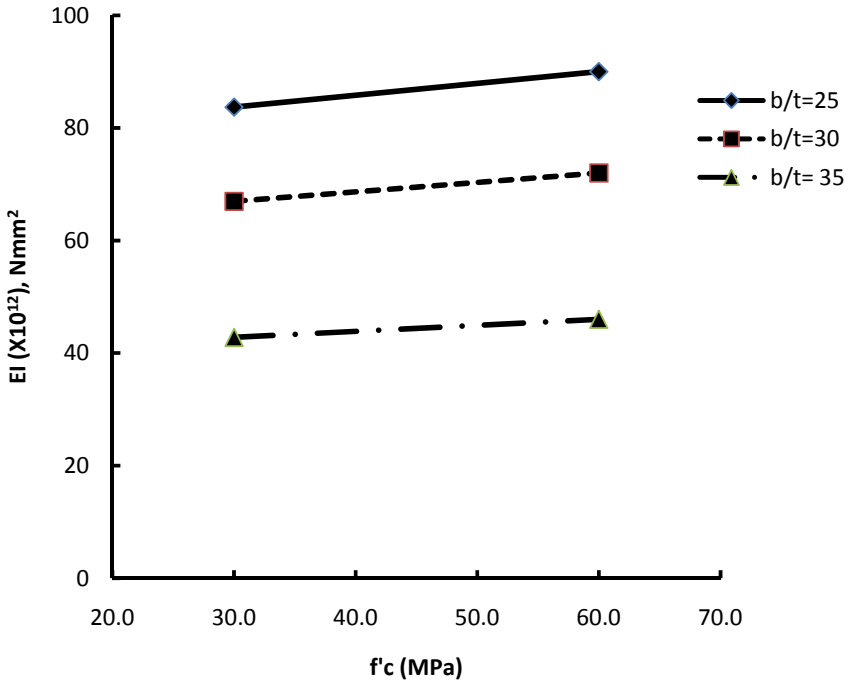

Figure 4.29 EI versus f'_c diagram for different values of b/t at e/d=0.4 (L/d =20, s/d=0.5 MPa and F_y=350 MPa.)

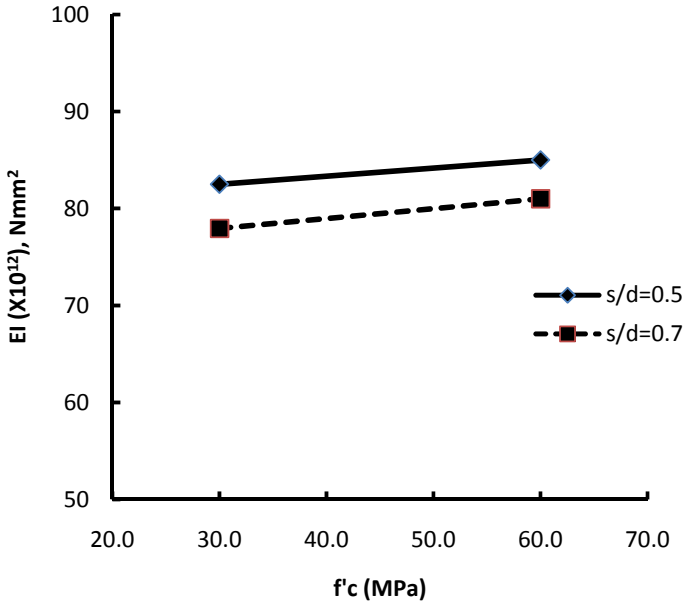

Figure 4.30 EI versus f'$_c$ diagram for different values of b/t at e/d=0.55 (L/d =20, b/t=30 MPa and F_y=350 MPa).

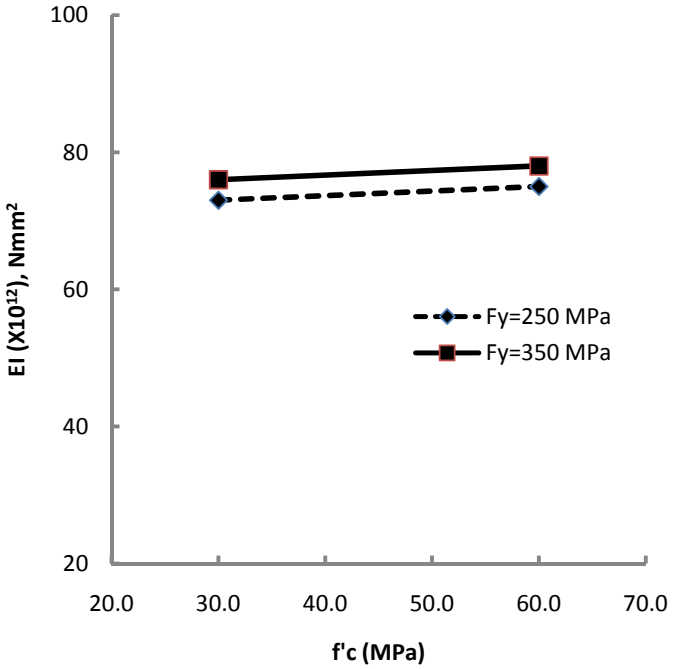

Figure 4.31 EI versus f'$_c$ diagram for different values of F_y at e/d=0.75 (L/d =20, b/t=30 MPa and s/d=0.5 MPa.)

Studying the graphs and observations on f'_c, it can generally be concluded that for all combinations with other parameters, effective flexural stiffness *EI* of the PEC column increases very little (maximum 6%) with increasing f'_c from 30 MPa to 60 MPa. However this increase in *EI* at high eccentricities (*e/d* = 0.55 and 0.75) as shown in Figures 4.30 and 4.31, is less than 3%. It is because of the fact that in high eccentricities i.e. high flexure, role of concrete in a PEC section becomes less significant as concrete is weaker in resisting flexural moment. In other words, the behaviour of slender columns are governed by stability not strength.

4.3.5 Effect of Yield Strength of Structural Mild Steel F_y

Yield strength of structural mild steel F_y contributes to both axial load carrying capacity and moment resisting capacity of a PEC column. Therefore F_y has an effect on the required cross sectional size of column for a particular combination of axial and flexural load. Therefore, F_y has been chosen as a parameter that may affect the flexural stiffness of PEC columns. In the parametric study F_y was varied from 250 MPa to 350 MPa to investigate its influence on *EI* of PEC columns in combination with other parameters.

Figure 4.32 shows variation of *EI* with F_y values for the different values of *L/d* at *e/d* = 0.4. Figure 4.33, 4.34 and 4.35 show the same variation for different values of *b/t, s/d and* f'_c respectively at random *e/d* ratios.

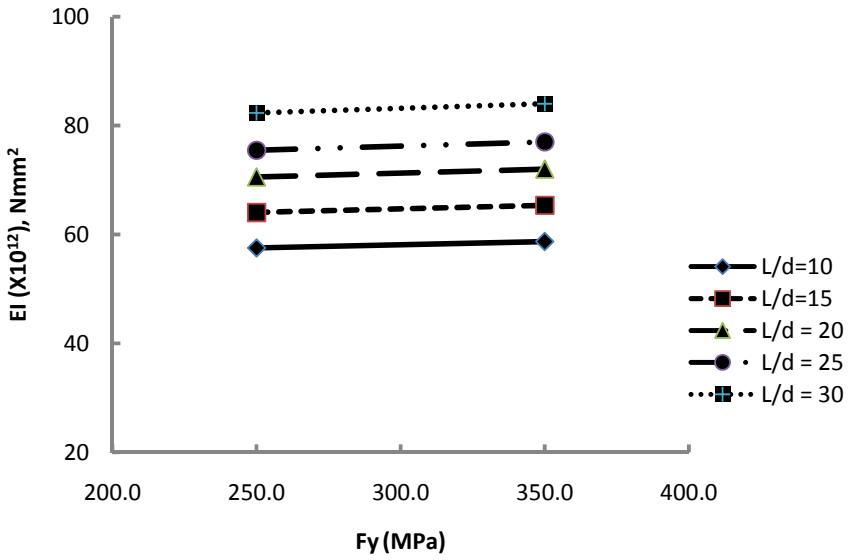

Figure 4.32 EI versus F_y diagram for different values of L/d at e/d=0.4 (b/t =25,s/d =0.5and f'_c=60 MPa)

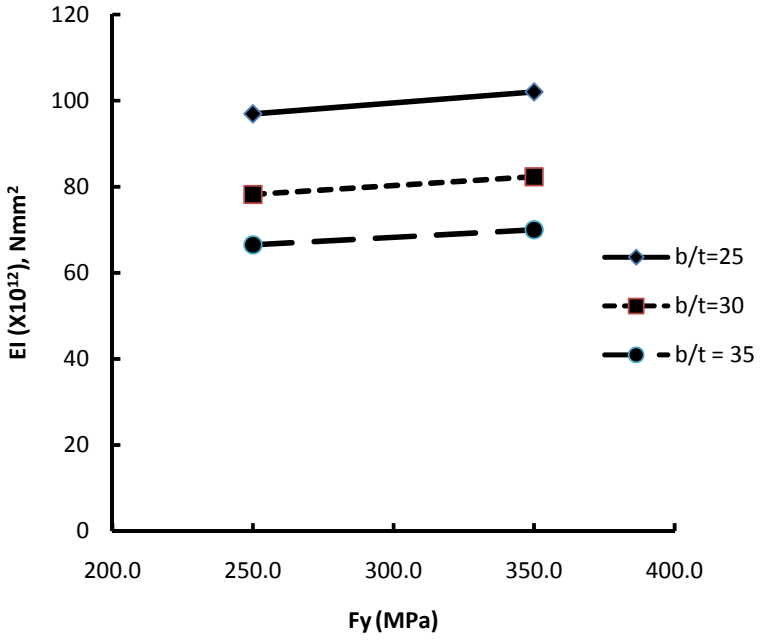

Figure 4.33 EI versus F_y diagram for different values of b/t at e/d=0.15 (L/d =20, s/d =0.5and f'_c=60 MPa)

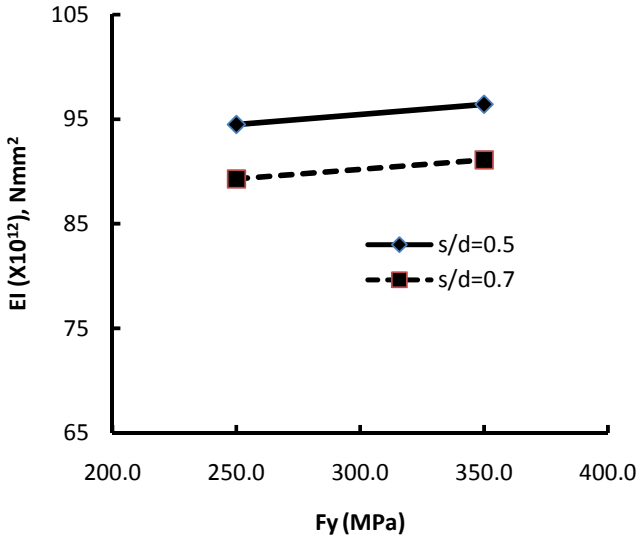

Figure 4.34 EI versus F_y diagram for different values of s/d at e/d=0.55 (L/d =25,b/t =25 and f'_c=60 MPa)

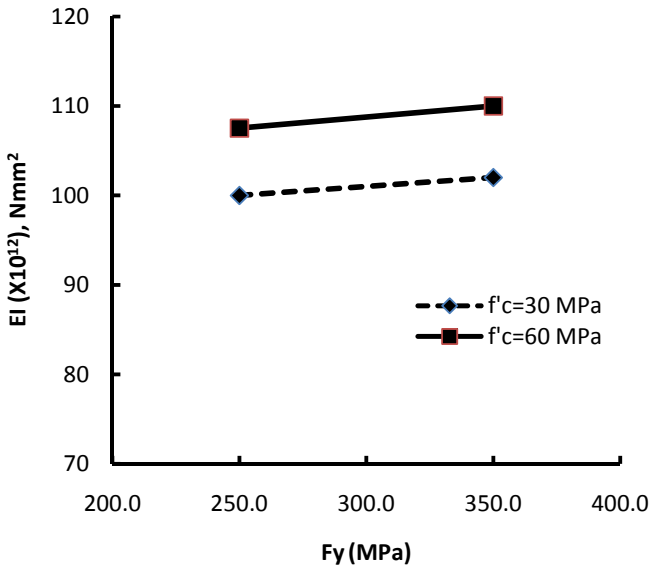

Figure 4.35 EI versus F_y diagram for different values of f'_c at e/d=0.2 (L/d =25,b/t =25 and f'_c=60 MPa)

From the figures it is evident that theoretical *EI* value is hardly affected with the change of F_y . All these graphical figures invariably show almost horizontally sloped curves which characterizes the triviality of the effect of yield strength (F_y) of structural steel shape on flexural stiffness (*EI)* of PEC columns. The reason behind this behaviour is that irrespective of the values of F_y, the modulus of elasticity of steel E_s remains the same. As a result flexural stiffness *EI* does not change noticeably with an increase in F_y.

Chapter 5

FORMULATION OF DESIGN EQUATION FOR FLEXURAL STIFFNES OF SLENDER PEC COLUMNS

5.1 COMPARISON OF THEORETICAL STIFFNESS DATA WITH ACI EQUATION

In the preceding chapter, a total number of 120 columns were simulated and studied for different individual combinations of the selected geometric and material parameters. Each of these columns was analyzed for the 10 specific *e/d* ratios. Therefore a total number of 1200 stiffness data were generated. As stated in section 3.2.2, the following expression of theory of elasticity derived from the secant formula for the theoretical flexural stiffness of a pin-ended column subjected to symmetrical single curvature bending is used for computation of the theoretical stiffness data.

$$EI_{th} = \frac{P_u l^2}{4\left[\sec^{-1}\left(\frac{M_{cs}}{M_{col}}\right)\right]} \qquad \ldots (3.11)$$

These theoretical stiffness values generated for all columns have been compared with their respective stiffness values calculated form ACI equation. As discussed in section 3.3, the following equation permitted by ACI Building code is used for calculating the effective flexural stiffness (EI_{ACI}) of slender composite columns

$$EI_{ACI} = 0.2E_cI_g + E_sI_{ss} \qquad \ldots (3.14)$$

Equation (3.14) was compared with the theoretical stiffness values (EI_{th}) computed from Equation (3.11) for all simulated composite columns.

The theoretical stiffness values (EI_{th}) and the stiffness values calculated from the ACI equation (EI_{ACI}) has been statistically analyzed. In order to determine the deviation between theoretical stiffness values (EI_{th}) from that of ACI equation (EI_{ACI}) a dimensionless stiffness ratio $\frac{EI_{th}}{EI_{ACI}}$ is introduced. Figure 5.1 shows a histogram for $\frac{EI_{th}}{EI_{ACI}}$.

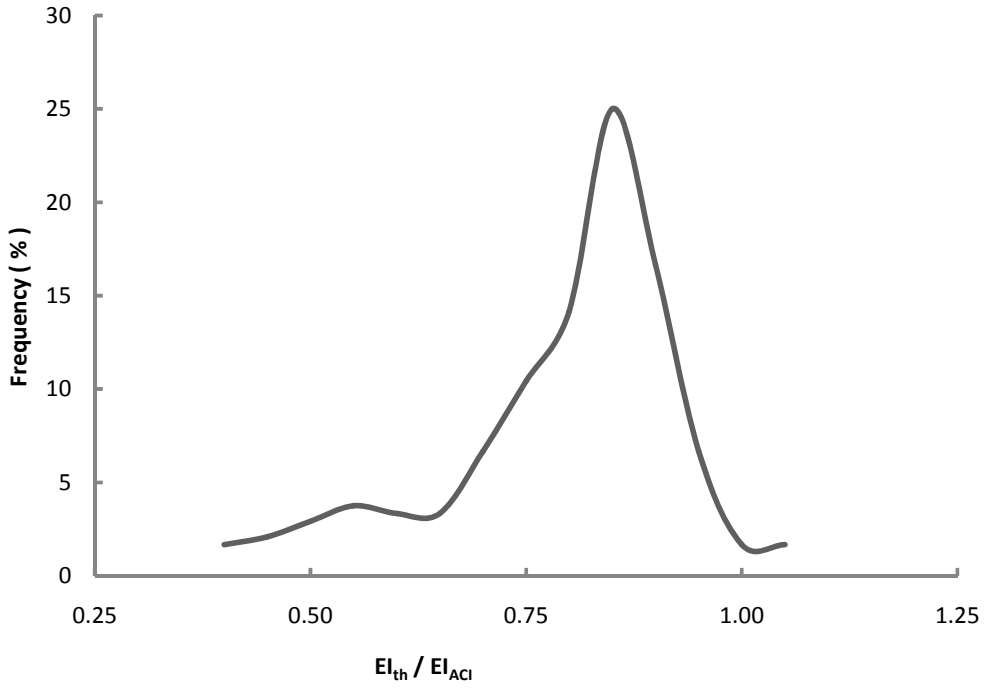

Figure 5.1: Histogram of the ratio of theoretical stiffness to ACI stiffness

Figure 5.1 shows that the mean value of stiffness ratio is 0.77 which is much lower than unity. On the average, the ACI values of *EI* are much higher than the theoretically predicted values of *EI* for slender PEC columns. For a significant number of columns studied, the theoretical *EI* substantially deviated from the ACI *EI* . This is because the ACI design equation was mainly developed for reinforced concrete columns and does not include all the parameters that may affect the stiffness of slender PEC columns. The histogram of EI_{th}/ EI_{ACI} in Figure 5.1 indicates that a modification in the ACI *EI* equation is required for PEC columns.

5.2 DEVELOPMENT OF THE PROPOSED DESIGN EQUATION

The variables that are most likely to affect the effective flexural stiffness of a slender PEC column have been discussed in the preceding chapter. An extensive parametric study is also performed in order to quantify the effect of the selected parameters and their inter relationships on the flexural stiffness (*EI*) of PEC columns. The parametric variables which have the greatest effect on *EI* have also been sorted out from the parametric study.

A linear regression analysis is performed using the parametric data for the development of a reasonably accurate and simple equation for *EI*. For this purpose the ACI equation for *EI* (Equation. 3.14) is intended to be modified by introducing multiplying factors to it. From the parametric study it was observed that the most important variables affecting *EI* are overall column slenderness ratio (*L/d)* and load eccentricity ratio (*e/d)*. Plate slenderness ratio (*b/t*) has also a significant effect. But for the sake of simplicity, only the first two prominent variables i.e. *L/d* and *e/d* are used for regression analysis for a single value of the third significant parameter *b/t*=25. For practical purpose the proposed equation may be used for a range of *b/t* varying from 22 to 26. Other less significant variables are kept constant at f'_c=60 MPa, F_y =350 MPa and *s/d*=0.70 for regression analysis. Therefore the proposed multiplying factor to the ACI equation becomes practically a function of *L/d* and *e/d* :

$$\frac{EI_{proposed}}{EI_{ACI}} = f(L/d, e/d)$$

Therefore, $EI_{Proposed} = f(L/d, e/d).EI_{ACI}$ … *(5.1)*

From regression analysis the expression for *f(l/d, e/d)* is as follows:

$$f(L/d, e/d) = \begin{cases} (0.024\ L/d - 0.90)\ e/d + 0.005\ L/d + 0.91 \text{ for } b/t = 25, \\ (0.023\ L/d - 0.85)\ e/d + 0.004\ L/d + 0.88 \text{ for } b/t = 30, \\ (0.022\ L/d - 0.84)\ e/d + 0.004\ L/d + 0.86 \text{ for } b/t = 35. \end{cases}$$

It is evident that the function *f(L/d, e/d)* varies a little (the variation is within 10%) for different values of *b/t*. So, for simplicity in practical design purpose, a generalized function will be chosen as the average of the above three functions for *f(L/d, e/d)*.

Therefore, replacing the expressions for *f(L/d, e/d)* and EI_{ACI} in Equation 5.1, the proposed design equation for flexural stiffness of PEC columns will take the form,

$$EI_{Proposed} = \{(0.023\ L/d - 0.85)\ e/d - 0.004\ L/d + 0.88\}(0.2E_cI_g + E_sI_{ss}) \quad \ldots(5.2)$$

$$[20 \leq b/t \leq 35]$$

5.3 VERIFICATION OF THE PROPOSED DESIGN EQUATION

In order to verify the accuracy of the proposed equation a limited comparative statistical analysis is performed. Figure 5.2 shows a histogram of the ratio between theoretical stiffness and stiffness from proposed equation.

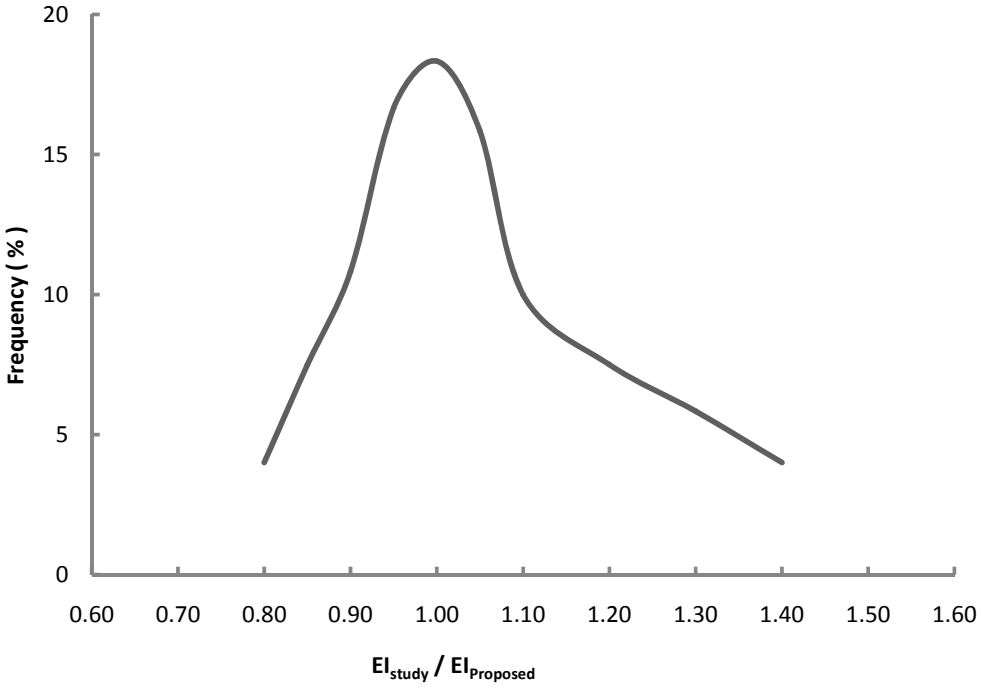

Figure 5.2: Histogram of theoretical stiffness with proposed stiffness equation

From Figure 5.2 it can be observed that the ratio $EI_{th}/EI_{proposed}$ has the maximum frequency around unity. The mean value of the $EI_{th}/EI_{proposed}$ is 1.10 which is much closer to unity than the mean value EI_{th}/EI_{ACI} . Therefore it can be said that the proposed *EI* equation is practically more accurate than the ACI equation within the specified range of parameters. This is due to the fact that for development of the proposed equation, the variables that are likely to affect the flexural stiffness *EI* of PEC columns have been taken into account which were not in the case of ACI equation.

Chapter 6

CONCLUSIONS AND RECOMMENDATIONS

6.1 INTRODUCTION

Partially encased composite (PEC) column is a comparatively new type of composite column which consists of a thin-walled welded I shaped steel section with transverse links welded between the opposing flanges that is infilled with concrete cast between the flanges. Experimental and numerical researches have been previously done to study the behaviour of short PEC columns under static and dynamic load. But no effective study has yet been done on the effective flexural stiffness *EI* of the PEC columns. Also, the influences of different geometric and material parameters on the slenderness behaviour of this kind of columns are yet to be investigated. Moreover, the ACI *EI* expressions for composite columns are quite approximate as they do not include all the parameters which are likely to affect the flexural stiffness of columns (Mirza and Tikka 1999).

An extensive parametric study has been conducted in this research in order to observe the effects of different parameters on the flexural stiffness *EI* of slender partially encased composite columns subjected to bending about the major axis of the steel section. The parameters which are likely to have the greatest effect on the behaviour of slender PEC columns were selected. A number of 1,200 parametric data regarding *EI* were generated in this study. In the parametric analysis, elastic strain compatibility and Newmark's method were used for computation of *EI*. The columns analysed were subjected to short-term loads and equal end moments causing symmetrical single-curvature bending about the major axis of the encased steel section.

Six parameters were chosen for the parametric study to investigate their effect on *EI* of PEC columns. The parameters are overall column slenderness ratio (*L/d*), initial load eccentricity ratio (*e/d*), flange plate slenderness ratio (*b/t*), link spacing-to-depth ratio (*s/d*), compressive strength of concrete (f'_c) and yield strength of structural steel plate

(F_y). From the parametric analysis, the influence of each different parameter on the flexural stiffness *EI* of the PEC column has been revealed. A statistical evaluation of the parameters that affect the flexural stiffness *EI* of slender partially encased composite columns has also been conducted. The existing ACI 318-02 equations were examined and a new nonlinear equation for *EI* was developed from the simulated data.

6.2 CONCLUSIONS

The major findings of the current study are summarised below:

- The theoretical stiffness for 120 PEC columns have been evaluated for different levels of load eccentricity ratio and in total 1200 stiffness data has been generated for PEC columns subjected to bending about major axis of the steel section. This extensive data base covers the wide range of four geometric (*L/d, e/d, b/t and s/d*) variables and two material variables ($f_c^{'}$ and F_y) affecting the behaviour of PEC columns.

- Among the six variables selected for this study the overall column slenderness ratio (*L/d) and* load eccentricity ratio (*e/d*) have been found to have the most significant effects on the flexural stiffness of PEC columns.

- Flexural stiffness (*EI)* of the PEC column increases with an increase in *L/d* ratio irrespective of the selected values of other variables. In general, *EI* increases around 1.5 times for changing *L/d* from 10 to 30. However, the rate of increase in EI is diminishes at higher *L/d* ratios (i.e., *L/d* ratio over 20).

- Effect of load eccentricity ratio on *EI* is studied with respect to the selected range of other variables (i.e. *L/d, b/t, s/d, f'*$_c$ and F_y). For all cases, *EI* decreases significantly with increasing *e/d* values. At higher eccentricities the rate of change in *EI* is higher than that at lower eccentricities.

- *EI* declines with an increase in flange plate slenderness (*b/t*) ratio. On an average *EI* decreases to around two third for changing *b/t* from 25 to 35.

- The selected range of link spacing to depth (*s/d*) ratio seemed to have negligible effect on flexural stiffness of PEC columns. The *EI* value seemed to decrease by

less than 8% due to the change in *s/d* ratio from 0.5 to 0.7.

- The two material parameters selected in this study found to have negligible effect on the flexural stiffness of PEC columns. Changing the concrete strength from 30 MPa to 60 MPa results in an average increase in the stiffness of PEC columns by 4%. Increasing the grade of the structural steel shape of PEC columns from 250 MPa to 350 MPa results in only 2% increase in the flexural stiffness of this column. Therefore, the effective flexural stiffness of slender PEC columns seemed to be independent of the material strength of its constituent members.

- The flexural stiffness (EI_{th}) values obtained in this study for 1200 parametric data have been compared to the existing flexural stiffness (EI_{ACI}) equation in ACI code for RC and composite columns. It has been found that the existing ACI equation gives satisfactorily close results at low eccentricities. But at high eccentricities, EI_{ACI} differ largely from EI_{th}. A regression analysis has been conducted and a design equation was proposed to calculate the flexural stiffness of PEC columns subjected to major axis bending. This proposed equation includes the most important parameters (*L/d* and *e/d*) that were proven to be most significant factors affecting the behaviour of PEC columns under major axis bending. The reliability of the proposed *EI* equation was then tested against all the parametric data and was found to be satisfactory.

6.3 RECOMMENDATION FOR FUTURE RESEARCH

The current study was only confined to developing the effective flexural stiffness of slender PEC columns subjected to symmetrical single curvature bending about its major axis. Future research works can be conducted for evaluating the effective flexural stiffness for columns subjected to bending about the minor axis of the steel section.

The moment magnification factor for this new composite system should be developed for different end moment conditions to calculate the design moment for slender PEC columns.

The numerical study has been accomplished for slender PEC column subjected to static

monotonic loading only. Additional study should be carried out on the behaviour of PEC column subjected to cyclic loading.

Only linear material property has been considered for this study. Future research can be executed considering material nonlinearity and the numerical method can be modified to include nonlinear material behaviour of concrete in future research.

The experimental database for studying the behaviour of slender PEC columns is limited. Future research should focus on extensive experimental investigations on slender PEC columns. The results of these investigations can be for further validation and applicability of the proposed design equation of *EI* for these columns.

REFERENCES

ACI (2002). "Building Code Requirements for Structural Concrete and Commentary." *ACI 318-02, American Concrete Institute*, Detroit, USA

ACI (2005). "Building Code Requirements for Structural Concrete and Commentary." *ACI 318-05, American Concrete Institute*, Detroit, USA.

ACI (2008). "Building Code Requirements for Structural Concrete and Commentary." *ACI 318-08, American Concrete Institute*, Detroit, USA.

Ali, S. and Begum, M. (2012). "Numerical Analysis of Slender Partially Encased Composite Columns", *International Journal of Science and Engineering Investigations*, Vol. 1, Issue 3, pp.58-65.

Ali. S. (2012). "Behaviour of Slender Partially Encased Composite Columns" M. Sc. Engg. Thesis, Department of Civil Engineering, BUET, Dhaka, Bangladesh.

Begum, M., Driver, R. G. and Elwi, A. E. (2007). "Finite Element Modeling of Partially Encased Composite Columns using the Dynamic Explicit Solution Method." *Journal of Structural Engineering, ASCE*, 133 (3), pp. 326-334.

Begum, M., Driver, R. G. and Elwi, A. E. (2007). "Numerical Simulation of the Behaviour of Partially Encased Composite Columns.", Department of Civil and Environmental Engineering, University of Alberta, Canada.

Bouchereau, R. and Toupin, J.-D. (2003). "Étude du Comportement en Compression-Flexion des Poteaux Mixtes Partiellement Enrobés." *Report EPM/GCS-2003-03*, Dept. of Civil, Geological and Mining Engineering, Ecole Polytechnique, Montreal, Canada.

Chen, W. F. and Lui, E. M. (1987). "Structural stability—Theory and implementation", Elsevier, New York.

Chicoine, T., Tremblay, R., Massicotte, B., Yalcin, M., Ricles, J., and Lu, L.-W. (2000). "Test Programme on Partially-Encased Built Up Three-Plate Composite Columns." *Joint Report EPM/GCS No. 00-06*, February, Dept. of Civil, Geological and Mining Engineering, Ecole Polytechnique, Montreal, Canada – ATLSS Engineering Research Centre, No. 00-04, Lehigh University, Bethlehem, Pennsylvania, USA.

Chicoine, T., Tremblay, R. and Massicotte, B. (2001). "Finite Element Modelling of the Experimental Response of Partially Encased Composite Columns." *EPM/GCS No. 2001-06,* Dept. of Civil, Geological and Mining Engineering, Ecole Polytechnique, Montreal, Canada.

Chicoine, T., Tremblay, R., Massicotte, B., Ricles, J., and Lu, L.-W. (2002a). "Behavior and Strength of Partially-Encased Composite Columns with Built Up Shapes." *Journal of Structural Engineering, ASCE*, 128 (3), pp. 279-288.

Chicoine, T., Tremblay, R. and Massicotte, B. (2002b). "Finite Element Modelling and Design of Partially Encased Composite Columns." *Steel and Composite Structures,* 2 (3), pp. 171–194.

Chicoine, T., Massicotte, B. and Tremblay, R. (2003). "Long–term Behavior and Strength of Partially-Encased Composite Columns with Built Up Shapes." *Journal of Structural Engineering, ASCE,* 129 (2), 141–150.

CSA. (2001). "CSA S16-01, Limit States Design of Steel Structures." Canadian Standards Association, Toronto, ON.

CSA. (2004). "CSA A23.3-04, Design of Concrete Structures." Canadian Standards Association, Rexdale, ON.

CSA. (2004). "CSA A23.3-04, Design of Concrete Structures." Canadian Standards Association, Rexdale, ON.

Elnashai, A.S., and Broderick, B.M. (1994). Seismic resistance of composite beam-columns in multi-story structures. Part 1: Experimental studies. Journal of Constructional Steel Research, Elsevier, Oxford, UK, 30, pp. 201-229

Filion, I. (1998) ″Étude Expérimentale des Poteaux Mixtes Avec Section d'acier de classe 4*”*, *Report n^{o}. EPM/GCS-1998-06,* Dept. of Civil, Geological and Mining Engineering, Ecole Polytechnique, Montreal, Canada.

Hunaiti, Y. M., and Fattah, B. Abdel (1994). "Design Considerations of Partially Encased Composite Columns." *Proc. Inst. Civ. Eng., Struct. Build., 106 (2),* pp. 75-82.

Maranda, R. (1998) "Analyses par Eldments Finis de Poteaux. Mates Avec Sections d'acier En I de Classe 4" *Report n°. EPMIGCS-1998-11,* Dept. of Civil, Geological and Mining Engineering, Ecole Polytechnique, Montreal, Canada.

Mirza, S. A. and Tikka, T. K.(1999) “Flexural stiffness of composite columns subjected to major axis bending”, ACI Structural Journal, 96(1), pp. 19-28

Mirza, S.A. (1990) “Flexural Stiffness of Rectangular Reinforced Concrete Columns”, American Concrete Institute Structural Journal, 87(4): 425-435.

Newmark, N. M. (1943) "Numerical Procedure for Computing Deflections, Moments, and Buckling Loads", ASCE, V. 108, pp. 1161-1234.

Plumier, A., Abed, A. and Tilioune, B. (1995). Increase of buckling resistance and ductility of H-sections by encased concrete. *Behaviour of Steel Structures in Seismic Areas: STESSA '94*, ed. by F.M. Mazzolani and V. Gioncu, E&FN Spon, London, pp. 211-220.

Prickett, B. S. and Driver, R. G. (2006). “Behaviour of Partially Encased Composite Columns Made with High Performance Concrete.” *Structural Engineering Report No 262*, Dept. of Civil and Environmental Engineering, University of Alberta, AB, Canada.

Tikka, T. K. and Mirza, S.A. (2006) “Nonlinear Equation for Flexural Stiffness of Slender Composite Columns in Major Axis Bending”, Journal of Structural Engineering, ASCE, Vol. 132(3), pp. 387-399.

Timoshenko, S.P. and Gere, J.M. (1961) “Theory of Elastic Stability”, 2nd Edition, McGraw-Hill Book Co., New York, N.Y., pp. 552.

Tremblay, R., Massicotte, B., Filion, I., and Maranda, R. (1998). “Experimental Study on the Behaviour of Partially Encased Composite Columns Made with Light Welded H Steel Shapes under Compressive Axial Loads.” *Proc., SSRC Annual Technical Session & Meeting*, Atlanta, 195-204.